EFFECT OF ALLOYING ELEMENT ON Al-12.6%Si EUTECTIC ALLOYS

Thesis submitted in partial fulfillment of the requirement for
The award of the degree of
Master of Technology
In
MATERIALS SCIENCE AND ENGINEERING

Submitted by

ALOK JAIN
Roll No.60602004

Under
The guidance of

Dr. O.P Pandey

School of Physics & Material Sciences
Thapar University, Patiala
Patiala - 147001
June-2008

Dedicated to my Family

CERTIFICATE

This is to certify that Mr. ALOK JAIN, Roll No. 60602004 has worked on this thesis report as a partial fulfillment for award of the degree of MASTERS OF TECHNOLGY in Material Science and Engineering. I certify that the matter embodied in this report is of the candidate's own record and not submitted to any other university in any part or full form for the award of such kind of a degree.

(Dr. O.P.Pandey)
Supervisor
SPMS, Thapar University
Patiala

Countersigned by:

Dr.O.P.Pandey
(Prof. & Head)
School of Physics and Materials Science
Thapar University, Patiala

Dr. R.K.Sharma
Dean of academic Affairs
Thapar University
Patiala

ACKNOWLEDGEMENT

No matter how much enterprising and entrepreneurial one's thinking is, yet nobody can do everything all by himself without some help and guidance. It is inhumane if the concerned person's assistance goes without appreciation and thanks. My first and foremost offering of thanks goes to the architect who shaped my dreams into reality, my guide and mentor **Dr. O.P Pandey**. Prof. and Head, School of Physics and Material Science, Thapar University, Patiala. Perseverance, exuberance, positive approaches are just some of the traits he imprinted on my personality. He steered me through his journey through his invaluable advice, positive criticism, stimulating discussion and consistent encouragement. His meticulous attention towards my proceedings, his devoted time and his ideas has enabled me to make the project a success. His faith in me has always made me more confident. It had been my privilege to work under his guidance.

I would like to thank **Dr. Kulvir Singh**, Assistant Professor, School of Physics and Materials Science for his full motivation and appreciation to my work. My greatest thanks to **Dr. Sanjeev Das**. He has been very helpful in improving. I am grateful to him for sharing his time and expertise. My special thanks to P G Lab incharge **Mr. Purushottam**. His assistance and partnership were of great pleasure. I would also like to thank **Mr. Jant Singh**, for providing all kind of assistance in PG Lab for creating a healthy research environment.

I would also like to give many thanks to Research Scholar **Ms. Kamalpreet Kaur** for any kind of help and valuable suggestions whenever I needed. All the faculties, my friends, and my colleagues at the Materials Science & Engineering program and the School of Physics and Material Sciences are acknowledged for providing me a friendly atmosphere and encouraging me throughout this research. **Thanks to my parents** who are always with me when I feel low and **special thanks to my little sister** who always boost my moral. Thanks to my would be wife **Ms. Neeru Sharma,** who inspired me to do more and more hard work to complete my work in time.

Alok Jain

Alok Jain

Roll No.60602004

ABSTRACT

Al-Si alloys are in demand for several structural devices because of their high strength to weight ratio. The enhancements in properties are further observed when suitably alloyed with the different elements. Al-Si alloy find their application mostly in automobile engineering. Alloys of eutectic composition are used as piston alloys as Si exhibit good wear properties. Si in the matrix nucleates as needle structure when solidified. These needle structures when modified exhibit very good thermal and wear properties.

In the present work attempt has been made to modify Al-Si eutectic microstructure by alloying it with certain amount of immiscible elements. These have been tried singly and as well as in combinations. It has been observed that all elements have tendency to modify the structure by adding as a barrier center for the growth of Si needles. However, in certain cases this growth is not up to the mark.

The idea behind this work was to see the effect of addition of immiscible alloys for the refinement of microstructure. The theory of homogenous nucleation proposed by Volmer and Creber (1925) state the nucleation phenomena is governed by surface and volume free energy. However, this theory could not be satisfied for alloy systems. In this entire work it was observed that the refinement of Si needles could be observed for all composition studied for Bi, Pb, Ca, Cd and Sn.

LIST OF TABLES

LIST OF FIGURES

LIST OF ABBREVIATIONS

FCC	Face Centered Cubic
DPH	Diamond-Pyramid Hardness Number
VHN	Vicker Hardness Number
KHN	Knoop Hardness Number
FSP	Friction Stir Processing
SEM	Scanning Electron Micrograph
LM13	Al-12%Si-1%Ni-0.8%Cu-0.6%Mg
GRF	Growth Restricting Factor
CX-type modifiers	Modifiers That Have Long Effective Term
YS	Yield Strength
UTS	Ultimate Tensile Strength
Wt	Weight
HRB	Rockwell Hardness on B scale
Al	Aluminum
Si	Silicon
Ca	Calcium
Bi	Bismuth
Sn	Tin
Pb	Lead
Cd	Cadmium
B	Boron
Be	Berium

CONTENTS

CHAPTER – 1

INTRODUCTION

1.1 ALUMINUM

Aluminum is a metal having atomic number 13 having FCC structure. The properties of aluminum which chiefly dedicate its use as an engineering material are its low relative density coupled with a reasonably high tensile strength when used in one of its alloyed forms. Since its relative density is only about one third that of steel its alloys are widely used in aero, automobile and constructional engineering. A combination of suitable alloying and heat-treatment can produce alloys which, suitable for many engineering applications.

1.2 PROPERTIES OF ALUMINUM

Aluminum becomes the common structural material because of following properties.

1. **Light weight:** Aluminum weight roughly one-third as most of common metals, but is one and half times as heavy as magnesium. It finds application to reduce the weight of component and structures, particularly connected with transport, especially with aerospace. High strength to weight ratio can be achieved in certain alloys, which shows marked response to age hardening.
2. **Ease of fabrication and machinability:** It can be easily cast, rolled to any desired thickness, stamped, drawn, spun, forged and extruded to all shapes.
3. **High resistance to atmospheric corrosion:** Due to thin, impermeable aluminum oxide layer on the surface it protect from further oxidation. The corrosion resistance can be further improved by anodizing, a treatment which artificially thickness the natural oxide film. Since aluminum oxide is very hard, a wear resistance is also increased by the oxide layer; and slightly porous nature of the surface of the film allows it to be colored with either organic or inorganic dyes. In this aspect high oxygen affinity is an asset.
4. **Conductivity:** It has good thermal as well as electrical conductivities. The fact that aluminum has over 50% of specific conductivity of copper means that, weight for weight; it is better conductor of electricity than copper

5. **High metallic luster:** Due to its high reflectivity aluminum used as the reflectors in photographic reflectors.
6. **Non magnetic and non-sparking:** It is non magnetic and non- sparking in nature.

1.3 ALLOYS

Pure metals are rarely used for engineering purpose except where high electrical conductivity, high ductility or good corrosion resistance are required. These properties are generally at a maximum value in pure metal, but such mechanical properties such as tensile strength. Yield point and hardness are improved by alloying. In most cases the manufacturer of an alloy involves melting two or more metal together and allowing the mixture to solidify in a suitable mould.

An alloy is a metallic solid formed by an intimate combination of a metal and one, or more than one metal and/or non-metal, but has metallic properties. The metallic atom must dominate in its composition, and metallic bond in its crystal structure.

Alloys are usually made by dissolving the alloying element in one another in liquid state. The parent metal, or solvent (base metal), in largest concentration, is melted first in crucible and the solid pieces of the alloy addition in weighted amounts are added in it followed by stirring to get it dissolved. At this stage the alloy should be single homogeneous liquid solution in the crucible. Some molten metal do not dissolve in each other but instead of two separate layers. Molten lead and molten zinc do not dissolve in each other completely. Such a combination of metals does not result in a useful alloy as on solidification. Thus the formations of a useful alloy require all the components at atomic level to mingle intimately together in the liquid state. Alloys frequently contain more than two elements. The metal which is present in largest proportion is often referred as the parent metal, or solvent or base metal, whilst the metal (non metal) in smaller proportion is called solute

If a liquid solution of two elements is allowed to solidify the atom move and rearrange them to come to thermo dynamical equilibrium among themselves. The structure of the solidified alloy depend upon nature of the alloying element such as they are

1. Indifferent to each other
2. Attract one another, or
3. Repel each other

If the atoms are indifferent to one another, they behave as if belonging to the same species. They get mixed up together so thoroughly that the alloy is homogeneous up to the atomic level. This results in a random solid solution.

If the dissimilar atoms attract each other, and if they are electrochemically similar, then they often form an ordered solid solution, or even super lattice. In such a structure, the species are arranged in some regular alternating pattern. True metal often form them. But if the two species differ a lot electrochemically, the bond between them become partly ionic, resulting in the formation of an inter-metallic compound. In extreme cases of this, when one element is highly electronegative, a true chemical compound is formed (it is no more metallic) If similar atoms attract each other more, then they tend to separate into distinct and different crystals joined by in between the grain boundaries. Some grains have more of one type of atoms, while other has more of other types. Such microscopically heterogeneous mixtures are called phase mixtures.

1.4 ALLOYS OF ALUMINUM [20]

Addition of alloying elements is made principally to improve mechanical properties such as tensile strength, hardness, rigidity and machinability, and sometimes to improve fluidity and other casting properties.

Aluminum alloys are used in both the cast and wrought conditions. Whilst the mechanical properties of many of them can be improved by precipitating hardening and addition of other elements. With the expansion of aluminum market many of new compositions has been introduced.

We can Aluminum alloys can be in the following.

1. Wrought alloys which are not heat treated
2. Cast alloys which are not heat treated
3. Wrought alloys which are heat treated
4. Cast alloys which are heat treated

The brief description is given below.

1.4.1 Wrought alloys which are not heat treated

The main requirements of alloys in this category are sufficient strength and rigidity in the work hardened state, coupled with the good corrosion resistance.

These alloys are widely used in manufacturing of panels for land-transporting vehicles. Here the corrosion resistance of aluminum-magnesium alloys is utilized, those with the higher magnesium value having an excellent resistance to sea water and marine atmosphere. The desire mechanical properties are produced by the degree of cold work applied in the final cold working operation, and these alloys are commonly supplied as soft, or having undergone varying degree of work hardening as denoted by h1 h2 h3 up to h8(full hard). The main disadvantage is that, once material has been finished to size, no further variation can be made in mechanical properties. These alloys have high corrosion resistance and ductility due to presence of entire solid solution in the structure

1.4.2 Cast alloys which are not heat treated

Alloys in this group are widely used in the form of general purpose and casting and die castings. They are used very rigidly; good corrosion resistance and fluidity in casting are of greater importance than strength. Undoubtedly the most widely used alloys in this class are those containing between 9.0% to 13.0% silicon, with occasionally small amount of copper. These alloys are of approximately eutectic composition, a fact which makes them eminent suitable as die casting alloys, since their freezing range will be small. Rather coarse eutectic structure can be refined by a process known as modification. This consists of addition of small amount of sodium to the melt just before casting. The effect is to delay the precipitation of silicon when the normal eutectic temperature is reached, and also cause a shift of the eutectic composition toward the right of equilibrium diagram fig 1.2.

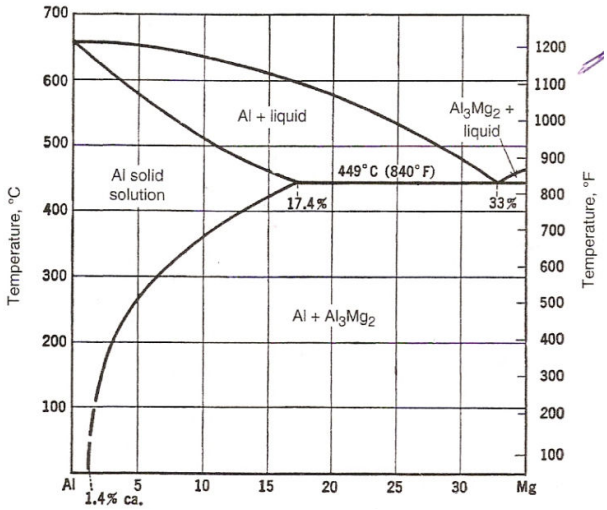

Fig 1.1 – Al-Mg phase diagram [18]

It is thought that the sodium collects in the liquid at the interface with the newly formed silicon crystal, inhibiting and delaying their growth. Thus undercooling occurs and new silicon nuclei are formed in large numbers resulting in a relatively fine grained eutectic structure. Remelting tend to restore the original structure due to a loss of sodium by oxidation. These aluminum-silicon alloys are better known as materials for die casting. Their high corrosion resistance makes these alloys useful for marine work, and the fact that they are somewhat lighter than aluminum-copper alloys makes them suitable for aero and automobile construction. Aluminum-copper alloys containing up to 10% copper popular.

These contained considerable amount of brittle compound $CuAl_2$ and were useful for rigidity and good casting properties and are required in the component not subjected to shock. They are also machinable but since their corrosion resistance was poor they have become complete obsolete.

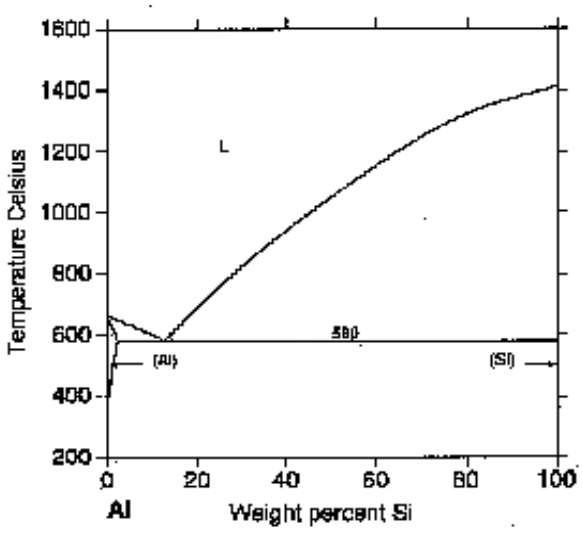

Fig 1.2 – Eutectic Al-Si phase diagram [18]

However, small amount of copper is added to the aluminum-silicon alloys to improve strength and machinability at the cost of some losses in castability and corrosion resistance. The main feature of the aluminum-copper phase diagram is precipitate hardening of alloys. The main feature of aluminum-magnesium-manganese alloy is good corrosion resistance which enables them to receive a high polish.

1.4.3 Wrought alloys which are heat-treated

Without doubt the most metallurgical-important feature of the aluminum alloys is the ability

of some of them to undergo a change in properties when heat treated suitably. Figure 1.3 shows Al-Cu phase diagram. Although this phenomenon is common to many alloys in which a change in solubility of some constituents in solvent metal takes place with variation in the temperature it is more widely used in suitable aluminum-base alloys than in others.

The age hardening process can be accelerated and higher strength obtained if the quenched alloy is heated at temperature up to 180^0C. Such treatment was known as artificial age hardening. Precipitation-hardening is not confined to the aluminum-base alloys, but can be applied to alloys of suitable composition from many systems in which a sloping phase boundary exists. As far as aluminum alloys are concerned, those containing copper,

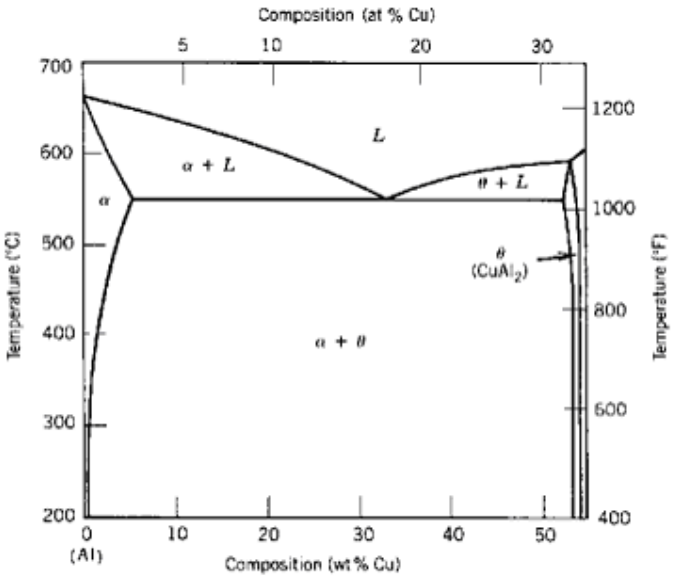

Fig 1.3 - Al-Cu phase diagram [18]

magnesium and silicon are the most important.In addition, precipitation-hardening is utilized in a number of magnesium-base alloys titanium alloys, some copper-base alloys and certain steels. Just as the application of heat will accelerate precipitation-hardening so will refrigeration impede the process. This fact was utilized extensively in aircraft production during Second World War. An alloy rivet must be of such a composition that it will age at ambient temperature, since it is inappropriate to precipitation-harden a completed airframe structure by any sort of furnace treatment. Unfortunately once solution-treated such a rivet will soon began to harden at harden at ambient temperature and if this hardening had begun any attempt to drive the rivet in this hard condition would cause it to split. Hence immediately after quenching from the Solution-treatment temperature, rivets were transferred to a refrigerator at about -20°C. By this means age-hardening was considerably slowed down

and rivet could be stored until required. Although the addition of copper forms the basis of many of the precipitation-hardening aluminum alloys, copper is absent from a number of them which rely instead on the presence of magnesium and silicon. Such alloys have a high electrical conductivity approaching that of pure aluminum, so that they can be used for the manufacture of overhead conductor of electricity.

1.4.4 Cast alloys which are heat-treated

One of the very successful alloys developed by N.P.L is still known by the series letter used to identify it during development-y alloy. Like Duralumin this is of the 4% copper type but contains also about 2% nickel and 1.5% magnesium. Precipitation-hardening is due to combined effects of coherent precipitation based on both $CuAl_2$ and $NiAl_3$, whilst fundamentally a casting alloy it can be used in wrought conditions.

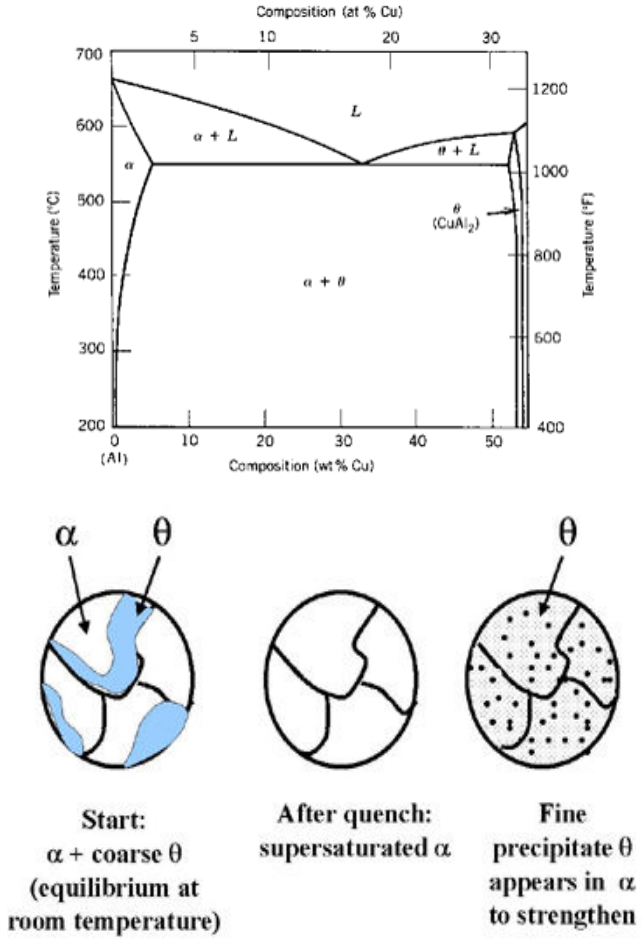

Fig 1.4 - Micro structural features on precipitation hardening

As a cast alloy it is useful where reasonable strength at high temperature is required, as in high duty pistons and cylinder heads for internal combustion engines. Its relatively low coefficient of expansion also makes it useful in this direction.

There are other casting alloys similar in composition to Y Alloy, but containing rather less copper. Some of these alloys can be precipitation hardened by heating at 155-170^{o}C without the usual preliminary solution treatment at a high temperature. This is due to sluggishness in precipitation of phase like $CuAl_2$ and $NiAl_3$ as the casting cools, following the initial pouring process. The 5.0 and 13.0% types of aluminum-silicon alloy are brought into this group by the addition of small amounts of either copper and nickel or magnesium and manganese, which render the alloys amenable to precipitation-hardening. Figure 1.4 showing precipitation hardening of Al-Cu alloy.

The use of aluminum-silicon alloys for automobile cylinder blocks has obvious advantages in term of weight saved as compared with the usual iron casting. Other advantages include higher thermal conductivity which assists heat transfer in the water cooling and lubrication systems, and enhanced corrosion resistance. Moreover, die casting can be used in the production costs when large numbers of castings are involved. Unfortunately the wear resistance of normal 11-13% silicon alloys is inadequate and cast iron liners need to be fitted resulting in increased cost.

Recently a range of hyper-eutectic aluminum-silicon alloys was developed. These contain 18-25% silicon and because of presence of large amount of primary silicon the wear resistance of these alloys is adequate for the use in cylinder blocks without the inclusion of cast iron liners. Both the wear resistance and mechanical strength of these alloys can be improved considerably by controlling the size and distribution of primary silicon. The finer and more evenly distributed primary silicon exhibites better the wear resistance. A number of methods have been proposed to refine this primary silicon and include the addition of small amounts of phosphorus, arsenic or sulphur to the melt just prior to casting. Since copper, magnesium and nickel are also present in sufficient quantities these alloys can be further hardened and strengthened by precipitation treatment. However, despite the advantage of the high silicon alloys production difficulties have presumably prevented them from becoming established even though established they are adequately covered in B.S 1490.

1.5 Hardness

The hardness of a material is a poorly defined term which has many meanings depending upon the experience of the person involved. In general, hardness usually implies a resistance to deformation, and for metals the property is a measure of their resistance to permanent or plastic deformation.

1.5.1 Vickers Hardness

The Vickers hardness test uses a square-base diamond pyramid as the indenter. The included angle between opposite faces of the pyramid is 136°. This angle was chosen because it approximates the most desirable ratio of indentation diameter to ball diameter in the Brinell hardness test.

Because of the shape of the indenter, this is frequently called the diamond-pyramid hardness test. The diamond-pyramid hardness number (DPH), or Vickers hardness number (VHN, or VPH), is defined as the load divided by the surface area of the indentation. In practice, this area is calculated from microscopic measurements of the lengths of the diagonals of the impression. The DPH may be determined from the following equation:

$$\mathbf{DPH} = \frac{\mathbf{1.854P}}{\mathbf{L^2}}$$

Where

P - applied load, kg

L - average length of diagonals, mm

1.5.2 Rockwell Hardness Test

The most widely used hardness test is the Rockwell hardness test. Its general acceptance is due to its speed, freedom from personal error, ability to distinguish small hardness differences in hardened steel, and the small size of the indentation, so that finished heat-treated parts can be tested without damage.

This test utilizes the depth of indentation, under constant load, as a measure of hardness. A minor load of 10 kg is first applied to seat the specimen. This minimizes the amount of surface preparation needed and reduces the tendency for ridging or sinking in by the indenter. The major load is then applied, and the depth of indentation is automatically recorded on a dial gage in terms of arbitrary hardness numbers.

The dial contains 100 divisions, each division representing a penetration of 0.00008 in (0.002 mm). The dial is reversed so that a high hardness, which corresponds to a small penetration, results in a high hardness number. This is in agreement with the other hardness numbers described previously, but unlike the Brinell and Vickers hardness designations, which have units of MPa, the Rockwell hardness numbers are purely arbitrary. Major loads of 60, 100, and 150 kg are used. Since the Rockwell hardness is dependent on the load and indenter, it is necessary to specify the combination which is used. This is done by prefixing the hardness, number with a letter indicating the particular combination of load and indenter for the hardness scale employed. A Rockwell hardness number without the letter prefix is meaningless.

Hardened steel is tested on the C scale with the diamond indenter and a 150-kg major load. The useful range for this scale is from about RC 20 to RC 70. Softer materials are usually tested on the B scale with a 1/16-in-diameter steel ball and a 100-kg major load. The range of this scale is from RB 0 to RB 100. The A scale (diamond penetrator, 60-kg major load) provides the most extended Rockwell hardness scale, which is usable for materials from annealed brass to cemented carbides. Many other scales are available for special purposes.

.

1.5.3 Microhardness Tests

Many metallurgical problems require the determination of hardness over very small areas. The measurement of the hardness gradient at a carburized surface, the determination of the hardness of individual constituents of a microstructure, or the checking of the hardness of a delicate watch gear might be typical problems. The development of the Knoop indenter by the National Bureau of Standards and the introduction of the Tukon tester for the controlled application of loads down to 25 g have made micro hardness testing a routine laboratory procedure. The Knoop indenter is a diamond ground to a pyramidal form that produces a diamond-shaped indentation with the long and short diagonals in the approximate ratio of 7:1 resulting in a state of plane strain in the deformed region. The Knoop hardness number (KHN) is the applied load divided by the unrecovered projected area of the indentation.

The special shape of the Knoop indenter makes it possible to place indentations much closer together than with a square Vickers indentation, e.g., to measure a steep hardness gradient. The other advantage is that for a given long diagonal length the depth and area of the Knoop indentation are only about 15 percent of what they would be for a Vickers indentation with the same diagonal length.

CHAPTER – 2

ALUMINUM-SILICON ALLOYS AND MODIFIERS

Most of the piston alloys used in industries are cast hypereutectic aluminum-silicon alloys. They have some very distinct advantages.

- Light-weight
- Low coefficient of thermal expansion
- low variation

Since the pistons are made to precise tolerances, the manufacturer needs to pour the alloy into the mold and have them solidified exactly the same way every time. An alloy with a composition near its eutectic will solidify almost all at once. An alloy that has a composition far from its eutectic will solidify at different rates with regard to the parts of each of the alloying elements. The precipitations of a hypereutectic alloy of Al-Si are an example of this but are tightly controlled to gain the desired properties and maintain low variation from one cast piston to another.

These advantages come from the properties of the hypereutectic alloy used. Thus, considering this fact that these exhibit good bearing properties, we have selected alloys of near eutectic composition but of hyper side.

2.1 Al-Si eutectic composition

Aluminum silicon foundry alloys are usually alloyed close to the eutectic or near eutectic compositions due to the small freezing range, good castability and desirable properties obtained at these compositions. As the molten alloy is cooled the silicon begins to come out of solution and form precipitates. Some of the silicon remains undissolvd in the matrix of aluminum. These little "islands" of silicon that are spread throughout the aluminum matrix greatly harden the metal and create a phenomenon known as precipitation hardening. They also cause a change in thermal properties resulting in a lower coefficient of thermal expansion and heat transfer.

Understanding the mechanism by which the eutectic forms and grows is important. During the solidification of aluminum silicon alloys, first the primary dendrites grow. After the dendrites impinge upon each other, the dendrite mobility is restricted. Mass transport to

compensate for shrinkage occurs mainly by interdendritic feeding. Interdendritic feeding involves the flow of eutectic liquid. Thus, the origin and growth of the eutectic is of major importance to fluid flow.

Figure 2.1 shows the microstructure of the aluminum-silicon eutectic. In general, when there are approximately equal volume fractions of the two phases, eutectics of binary alloys exhibit a lamellar structure. On the other hand, if one phase is present in a small volume fraction, this phase tends to be fibrous. As a rule of thumb, the eutectic microstructure obtained will tend to be fibrous when the volume fraction of the minor phase is less than 0.25, otherwise it will tend to be lamellar. If both phases in the eutectic are non-faceted, the eutectic will exhibit a regular morphology. In this case, the microstructure is made up of either lamellae or fibers having a high degree of regularity and periodicity. On the other hand, if one phase is faceted, the eutectic morphology is often irregular. Even though the volume fraction of silicon in the aluminum-silicon binary is less than 0.25, the typical aluminum-silicon eutectic is closer to a lamellar structure than to a fibrous one. This is usually attributed to the strong anisotropy of growth of silicon and to the relatively low interfacial energy between silicon and aluminum. Primary silicon is the pre-eutectic silicon formed in hypereutectic aluminum-silicon alloys.

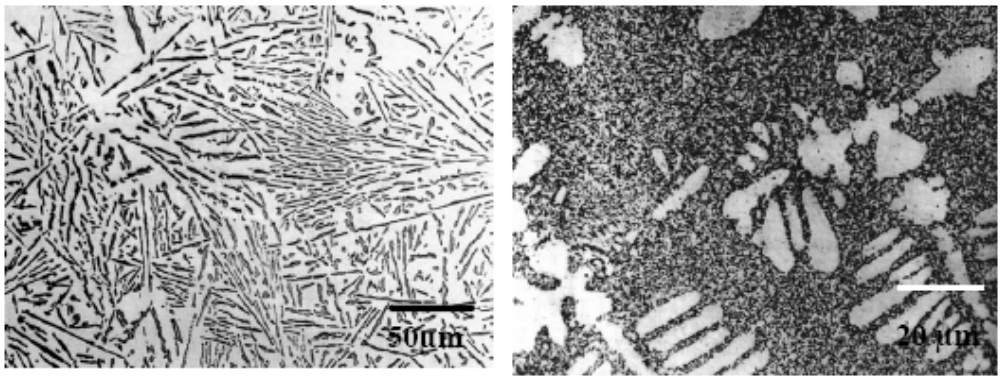

Figure 2.1: Al-12.5wt% Si alloy **(a)** Slowly cooled 200X **(b)** Chill Cast 500X

Primary silicon tends to assume different morphologies like massive crystals of geometric star like or dendritic shape, complex regular silicon morphology. Figure 2.2 gives the idea about how silicon needle morphology in the aluminum matrix at eutectic composition in scanning electron micrograph.

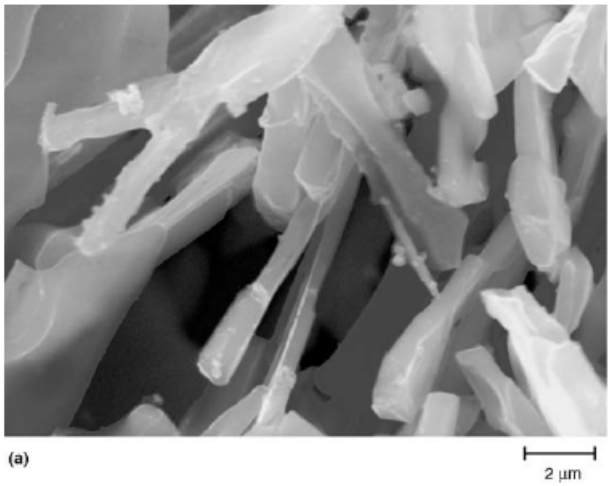

Figure 2.2: SEM of silicon needle in aluminum eutectic composition.

2.2 Effect of alloying elements on Al-alloys

The important alloying elements which are listed here are used as alloying elements in the casting of aluminum silicon casting alloys. Some of the effects, particularly with respect to impurities, are not well documented and are specific to particular alloys or conditions.

1. **Bismuth**: The low-melting-point metals such as bismuth, lead, tin, and cadmium are added to aluminum to make free-machining alloys. These elements have a restricted solubility in solid aluminum and form a soft, low-melting phase that promotes chip breaking and helps to lubricate the cutting tool. An advantage of bismuth is that its expansion on solidification compensates for the shrinkage of lead. A 1-to-1 lead-bismuth ratio is used in the aluminum-copper alloy, 2011, and in the aluminum-Mg-Si alloy, 6262. Small additions of bismuth (20 to 200 ppm) can be added to aluminum-magnesium alloys to counteract the detrimental effect of sodium on hot cracking.

2. **Cadmium**: is a relatively low-melting element that finds limited use in aluminum. Up to 0.3% Cd may be added to aluminum-copper alloys to accelerate the rate of age hardening, increase strength, and increase corrosion resistance. At levels of 0.005 to 0.5%, it has been used to reduce the time of aging of aluminum-zinc-magnesium alloys.

3. **Calcium:** has very low solubility in aluminum and forms the intermetallic $CaAl_4$. An interesting group of alloys containing about 5% Ca and 5% Zn have super plastic properties. Calcium combines with silicon to form $CaSi_2$, which is almost insoluble in aluminum and therefore will increase the conductivity of commercial-grade metal slightly. In aluminum-magnesium-silicon alloys, calcium will decrease age hardening. Its effect on aluminum-silicon alloys is to increase strength and decrease elongation, but it does not make these alloys heat treatable.

4. **Lead:** Normally present only as a trace element in commercial-purity aluminum, lead is added at about the 0.5% level with the same amount as bismuth in some alloys (2011 and 6262) to improve machinability.

5. **Tin:** It normally acts as the grain refiner. It helps to refine grain structure of the Al-Si eutectic alloys.

CHAPTER – 3
ALUMINUM SILICON CASTING TECHNIQUES

Aluminum is one of the few metals that can be cast by all of the processes used in casting metals. These processes, in decreasing order of amount of aluminum casting, are: die casting, permanent mold casting, sand casting (green sand and dry sand), plaster casting, investment casting, and continuous casting. Other processes such as lost foam, squeeze casting, and hot isostatic pressing are also mentioned.

There are many factors that affect selection of a casting process for producing a specific aluminum alloy part. The most important factors for all casting processes are:

- Feasibility and cost factors
- Quality factors.

In terms of feasibility, many aluminum alloy castings can be produced by any of the available methods. For a considerable number of castings, however, dimensions or design features automatically determine the best casting method. Because metal molds weigh from 10 to 100 times as much as the castings they are used in producing, most very large cast products are made as sand castings rather than as die or permanent mold castings. Small castings usually are made with metal molds to ensure dimensional accuracy. Quality factors are also important in the selection of a casting process. When applied to castings, the term quality refers to both degree of soundness (freedom from porosity, cracking, and surface imperfections) and levels of mechanical properties (strength and ductility). However, it should be kept in mind that in die casting, although cooling rates are very high, air tends to be trapped in the casting, which gives rise to appreciable amounts of porosity at the center. Extensive research has been conducted to find ways of reducing such porosity; however, it is difficult if not impossible to eliminate completely, and die castings often are lower in strength than low-pressure or gravity-fed permanent mold castings, which are sounder in spite of slower cooling.

Certain advantages are inherent in the metal casting process. These often form the basis for choosing casting over other shaping processes such as machining, forging, welding, stamping, rolling, extruding, etc. Some of the reasons for the success of the casting process are:

1. The most intricate of shapes, both external and internal, may be cast. As a result, many other operations, such as machining, forging, and welding, can be minimized or eliminated.
2. Because of their physical properties, some metals can only be cast to shape since they cannot be hot-worked into bars, rods, plates, or other shapes from ingot form as a preliminary to other processing.
3. Construction may be simplified. Objects may be cast in a single piece which would otherwise require assembly of several pieces if made by other methods.
4. Metal casting is a process highly adaptable to the requirements of mass production. Large numbers of a given casting may be produced very rapidly. For example, in the automotive industry hundreds of thousands of cast engine blocks and transmission cases are produced each year.
5. Extremely large, heavy metal objects may be cast when they would be difficult or economically impossible to produce otherwise. Large pump housing, valves, and hydroelectric plant parts weighing up to 200 tons illustrate this advantage of the casting process.
6. Some engineering properties are obtained more favorably in cast metals. Examples are:

   a) More uniform properties from a directional standpoint; i.e., cast metals exhibit the same properties regardless of which direction is selected for the test piece relative to the original casting. This is not generally true for wrought metals.

   b) Strength and lightness in certain light metal alloys, which can be produced only as castings.

   c) Good qualities are obtained in casting metals.

A decided economic advantage may exist as a result of any one or a combination of points mentioned above. The price and sale factor is a dominant one which continually weighs the advantages and limitations of process used in a competitive of enterprise.

3.1 Basic steps of casting

Three steps are involved in a casting process:

1) Heating metal till it becomes molten

2) Pouring the molten metal into a mould

3) Allowing the metal to cool and solidify in the shape of the mould.

3.2 Types of castings

1. Die Casting
2. Permanent mold casting
3. Evaporative (lost-foam) pattern casting
4. Shell Mold Casting
5. Plaster Casting
6. Investment casting
7. Centrifugal Casting
8. Continuous Casting
9. Composite-Mold Casting
10. Hot isostatic pressing
11. Hybrid Permanent Mold Processes

3.3 Defects in castings

During solidification of liquid metals and alloys, crystals formation takes place. The resulting morphology has certain characteristics peculiar to cast structures. Morphology includes both macrostructure and microstructure.

1. **Grain size effect:** During solidification process the grain size of cast product is quite large. For better strength we need to obtain the smaller grain size of the cast product.
2. **Grain boundary segregation:** Certain alloying substance should be added in the molten metal to correct its composition as well as react with unwanted substances. In some cases a fine distribution of brittle phase helps in enhancing properties however if these are segregated along the grain boundaries it may lead to failure of the cast product.
3. **Distribution in grain:** In certain cases where fine distribution is not possible they get segregated as a thick molten liquid in the entire mass through out the structure within the grain. This phase is brittle in nature and also has different coefficient of

thermal expansion as compared to matrix. This type of segregation if exists in higher scale may cause severe type of damage. In almost all type of castings certain unwanted phases exists because of their difference coefficient if thermal expansion. These phases may chip out easily and substance becomes weak from those areas.

4. **Cavities:** Blowholes, pinholes, smooth-walled cavities are some defects observed in casting. The largest cavities are most often isolated; the smallest (pinholes) appear in groups of varying dimensions. The interior walls of blowholes and pinholes can be shiny, more or less oxidized or, in the case of cast iron, can be covered with a thin layer of graphite. The defect can appear in all regions of the casting.
5. **Inclusions:** Number of additional compounds can be considered inclusions in cast structures. All aluminum contains aluminum carbide (Al_4C_3) formed during reduction. Borides may also be present. By agglomeration, borides can assume sufficient size to represent a significant factor in the metal structure, with especially adverse effects in machining.
6. **Porosity:** Porosity is a casting defect that typically appears as a network of small voids in the various region of the casting. If the porosity can be seen by the naked eye it refers to as macro porosity, while porosity that requires magnification is called micro porosity. Porosity caused by entrapment of gas bubbles in solidifying alloy. Porosity reduce the properties of the material.

CHAPTER – 4

LITRETURE REVIEW

Aluminum-silicon alloys have great importance in the industry due its physical and metallurgical properties. In industries the major draw back of the Al-Si alloys that they have needle like silicon particles imbedded in the aluminum matrix (fig 4.1). Due to presence of the coarse silicon particles in the aluminum, wear properties of the aluminum-silicon alloys decreases to appreciable extent. These particles although increase the strength of the material but increase the brittleness of the aluminum-silicon alloys and decrease the fracture toughness of these alloys. Since aluminum is one of the abundant metals found in earth and also have light weight, due to these properties we can use this metal to challenge the materials for high strength and good wear properties.

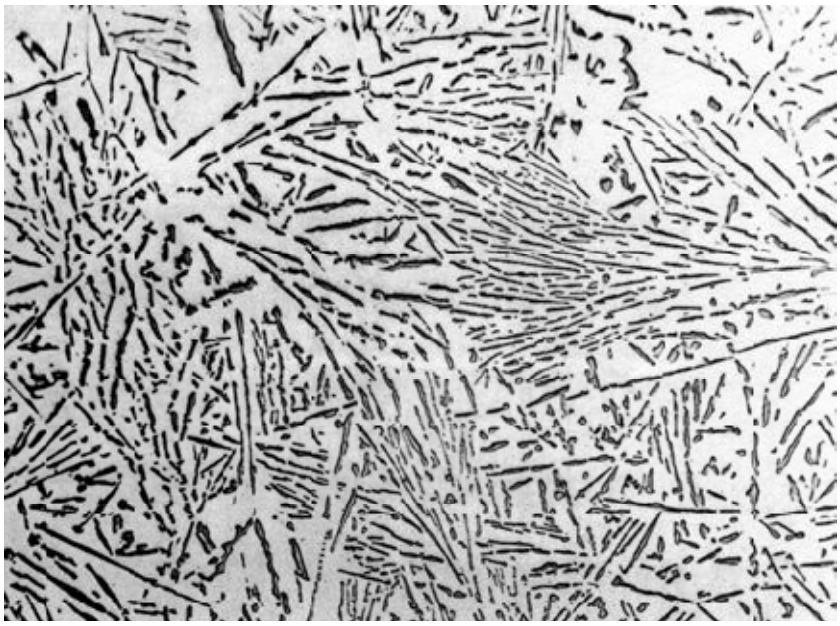

Fig 4.1-Al alloy having 12.5 wt% of si

4.1 Li Xin-tao et. al. [1] has reported one method of ultrasonic treatment of aluminum silicon alloy to reduce the particle size of silicon in the melt.

According to Li Xin-tao tundish metallurgy is a new concept that was first put forward to improve melt quality. The investigation of the relationship between tundish metallurgy and the product quality has been carried out, which has become a hot topic in

recent years. Ultrasound is a high frequency mechanical wave. The propagation and interaction of sound waves change the physical and chemical properties of materials that are subjected to ultrasound. Over the last few years high-intensity ultrasound has been used for producing new materials successfully. For example, ultrasonic treatment is applied in melts during solidification in order to obtain fine-grain solidification microstructures. High-intensity ultrasound has been used to fabricate continuous fiber and particulate reinforced metal matrix composites, by improving the wettability or promoting the chemical reaction between the reinforcement and the metal matrix.

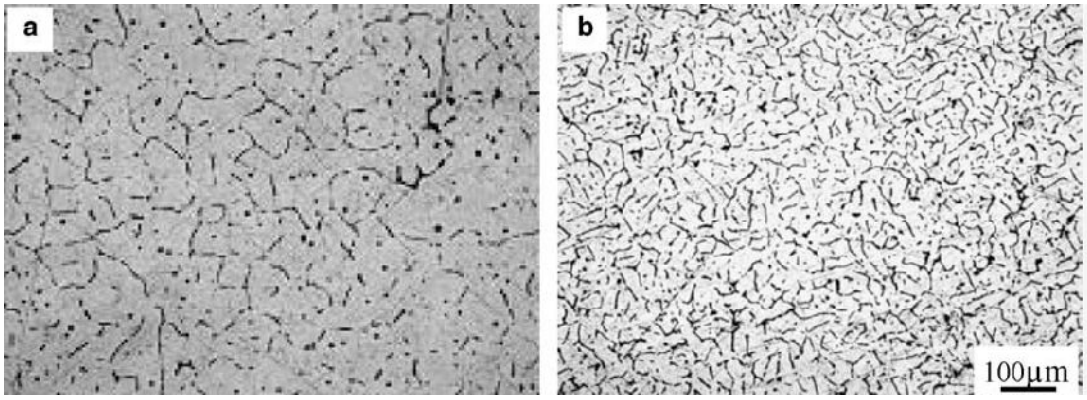

Fig 4.2 - Solidification structure of Al–1%Si cast ingots: (a) P = 0, (b) P = 1000W. [1]

Ultra sonic vibration helps to break the silicon flakes by increasing the power of vibrator according to limits. Figures 4.2 here shown the effect of waves on the aluminum silicon alloys and their microstructure ultrasonic melt treatment can significantly refine the solidification structure and suppress the boundary segregation of the Si element.

4.2 Z.Y. MA et. al. [2] have reported another mechanical method of grain refinement called stir casting method of grain refinement.

However, some mechanical properties of cast alloys, in particular, ductility, toughness, and fatigue resistance, are limited by three micro structural features: porosity, coarse acicular Si particles and coarse primary aluminum dendrites. **Friction stir processing (FSP)** has been applied to cast aluminum alloy A356 plates to enhance the mechanical properties through micro structural refinement and homogenization. The effect of tool geometry and FSP parameters on resultant microstructure and mechanical properties was investigated. The FSP broke up and dispersed the coarse acicular Si particles creating a uniform distribution of Si particles in the aluminum matrix with significant micro structural refinement. Further, FSP healed the casting porosity. These micro structural changes led to a

significant improvement in both strength and ductility. Higher tool rotation rate was the most effective parameter to refine coarse Si particles, heal the casting porosity, and consequently increase strength. Maximum strength was achieved at a tool rotation rate of 900 rpm and traverse speed of 203mm/min. Post-FSP aging increased strength for materials processed at higher tool rotation rates of 700 to 1100 rpm, but exerted only a marginal effect on samples prepared at the lower rotation rate of 300 rpm. Two-pass FSP with 100 pct overlapping passes resulted in higher strength for both as-FSP and post-FSP aged conditions.

4.3 Peter Szarvasy et. al. [3] reported that silicon phase in the aluminum alloys can also be modified by rapid solidification without modifiers.

The cooling rate has a significant influence on the modification process. The result of a high cooling rate is the appearance of a large number of crystallization centers, the growth of a number of particles, and a decrease in the interparticle spacing and modification of the phase. But at the same time there is an increase in the structural inhomogenity with the

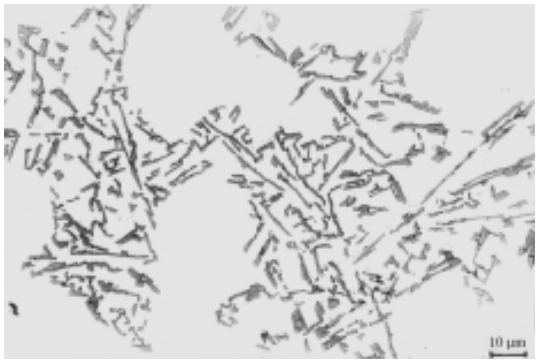

Fig 4.3 Cooling rate 2 Ks^{-1}, without modifier [3]

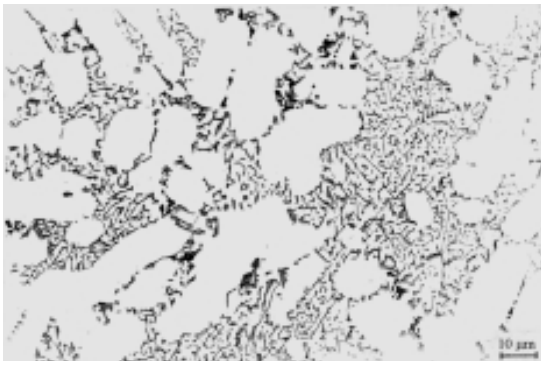

Fig 4.4 Cooling rate 18 Ks^{-1}, without modifier[3],

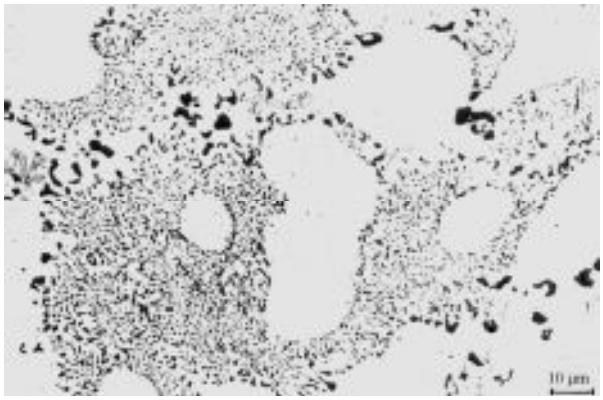

Fig 4.5 Cooling rate 2 Ks^{-1}, initial Sr content 0,015%, cast 24 hours after modifier applying,

appearance of "over-modified islands" which contain fine particles (less than 1 μm) and blowholes. Low cooling rates result in a coarse β phase as well as blowholes. Fig 4.3 showing cooling rate 2 Ks^{-1}.

A cooling rate above 14 Ks^{-1} results in a modification of the phase without a modifier (fig 4.4). A reduction of the cooling rate results in the growth of the number of needle-shaped particles which i.e. related to decrease in the mechanical properties. In the case of a cooling rate of 2 Ks^{-1} which corresponds with the cooling rate using a sand mould, the morphology of the phase is needle shaped with larger needles observed with a slower cooling rate (fig 4.5).

4.4 Xiufang Bian et. al. [4] reported that structural of silicon can also be modified by thermal treatment method.

The so-called thermal-rate treatment of alloy melt is such a technology that the melt is first superheated to a very high temperature, usually more than 300°C above its liquidous, keeping the temperature for several minutes, and then cooled quickly to a pouring temperature prior to pouring. By use of the thermal-rate treatment, the primary silicon grains in hypereutectic Al–Si alloys are remarkably refined.

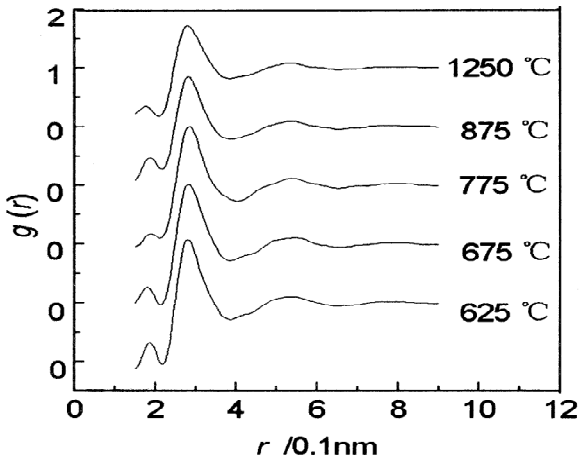

Fig 4.6 Pair correlation function *g*(r) of the Al–13 wt.% Si alloy. [4]

Fig 4.6 depicts the pair correlation function *g*(r) of the Al–13 wt.% Si alloy in the range from 625°C to 1250°C, the horizontal axes is the distance *r* of one atom to the reference atom, whereas the vertical axes is the appearance possibility of the atom at *r*. The height of the two peaks has a nonlinearity decrease and their positions have not any change with increasing temperature. With increasing temperature up to 775°C, the decrease of the height of peaks suggests that the break of the bonds happens in the melt and that Si atoms diffuse from Si–Si

cluster into the Al bulk melt. During the diffusion process, some original Si-Si bonds are destroyed, at same time some new Al-Si bonds have been formed. In the temperature range from 625^{o}C to 775^{o}C, the decrease of the peak height is not obvious; meaning the amount of the destroyed bond is close to that of produced bonds. At the same time, the coordination number of the melt increased slightly up to 11.30. While coordination number of pure liquid Al and Si is 11.5 and 4.8–5.8, respectively. From this fact, it can be deduced that the Si atoms occupied

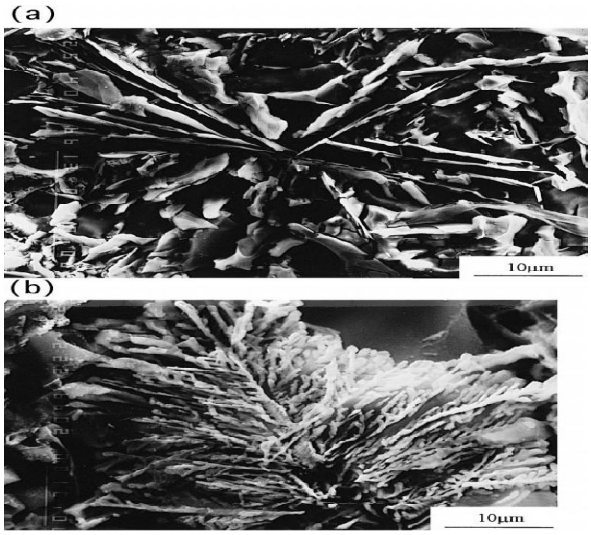

Fig 4.7 a & b SEM micrograph of the morphology of the Al–13 wt.% Si alloy. [4]

Fig 4.7a shows the scanning electron micrograph (SEM) of the morphology of coarse flake forms eutectic silicon in the Al–13 wt. % Si alloy that was heated only to 750^{0}C and poured into a cast iron mould. Fig 4.7b is the SEM micrograph of silicon in the alloy obtained by the thermal-rate treatment.

4.5 S.A. Kori et. al. [5] have reported the effect of grain refiner and or modifier on the wear behavior of hypoeutectic (Al–0.2, 2, 3, 4, 5 and 7Si) and eutectic (Al–12Si) alloys has been investigated using a pin-on-disc machine.

Al–Si alloys (0.2, 2, 3, 4, 5, 7 and 12 wt%Si) were prepared by using a commercial purity aluminum (99.7%) and Al–20 wt%Si master alloy. Melting of the alloy was carried out in a resistance furnace under a cover flux (45%NaCl + 45%KCl + 10%NaF) and the melt was held at 720^{o}C. After degassing with solid hexachloroethane (C_2Cl_6), master alloy chips (Al–Ti–B) duly packed in an aluminum foil were added to the melt for grain refinement. For

modification, Al–10%Sr master alloy was used. The melt was stirred for 30 s with zirconia coated steel rod after the addition of grain refiner and/or modifier, after which no further stirring was carried out. Melt were poured at 0 min and 5 min into cylindrical graphite mould (25mm diameter and 100mm height) surrounded by fire clay brick with it is top open for pouring.

Results suggest that, the specific wear rate decreases after the addition of grain refiner (1.0% M13) and or modifier (0.02%Sr) to the Al–7Si alloy compared to the absence of grain refiner and or modifier and confirms the experimental results. Thus, addition of grain refiner to Al–7Si alloy leads to increase in toughness and strength due to the structural changes from coarse columnar α-Al dendrites into fine α-Al dendrites, which leads to decrease in specific wear rate.

In an unmodified condition, the plate like eutectic Si acts as internal stress raiser in the microstructure and provides easy path for fracture. Modification (0.02%Sr) of Al–7Si alloy changes the microstructure from plate like eutectic Si to fine rounded particles. The change in morphology of Si reduces stress concentration at particle matrix interface and increases bonding of silicon crystals with soft eutectic matrix. Due to which the wear properties of Al–7Si alloy increases significantly compared to the absence of modifier.

4.6 LI Wei et. al. [6] studied the effect of barium on the refinement of primary aluminum and eutectics in hypoeutectic Al-Si alloys.

Barium was added as a master alloy in the range of 0.04%-0.08% retained Ba. Final barium concentration was verified by X-ray fluorescence analysis. The alloy was melted in an electric furnace with a graphic crucible in the laboratory (7.5 kW), but with a cast iron crucible in the foundry (30 kW). The typical experimental procedure consisted of melting the

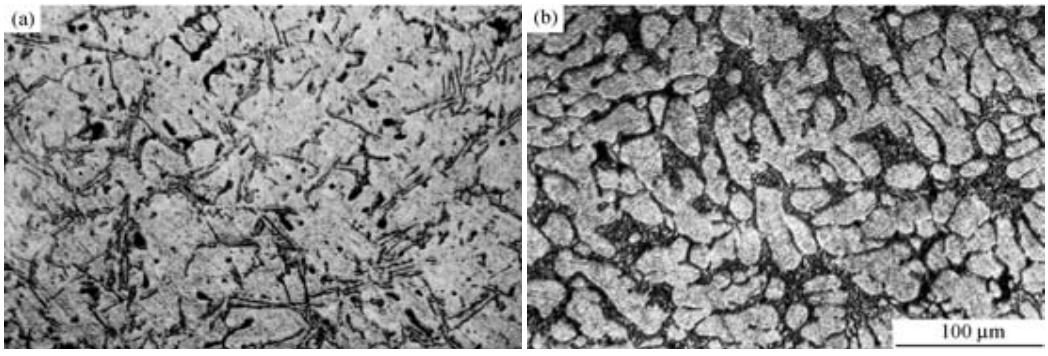

Comparision with a non-modified microstructure shown in **fig 4.8a**, a typical modified one is illustrated in **fig 4.8b**. [6]

alloy, adding the modifier, holding for 50 min with occasional stirring, and then degassing with either nitrogen (in lab.) or argon (in foundry) for 10 min before pouring. The degassing temperatures were kept among 700-720^{o}C, holding temperatures among 740-760 ^{o}C, and pouring temperature at about 750^{o}C. The permanent moulds were preheated to 300 ^{o}C for each pour.

As expected, the eutectic silicon is modified efficiently by barium additions. Figure 4.8a depicting non modified microstructure and figure 4.8b showing modified structure with Ba. As a better modifier of the hypoeutectic Al-Si alloy, barium can not only modify the eutectics but also refine the primary aluminum. Application of barium to the commercial hypoeutectic Al-Si alloy is reliable, and an even longer holding time can be taken when barium is used.

4.7 A.K. Prasada Rao et. al. [7] reported that under dry sliding condition. Al–7Si alloy was grain refined using various grain refiners such as Al–1Ti–3B, Al–3Ti and Al–3B while Al was grain refined with Al–5Ti–1B. The results suggest that the wear properties are not dependent on the type of grain refiner used, but depend on the grain size fig 4.9 showing effect of refiners.

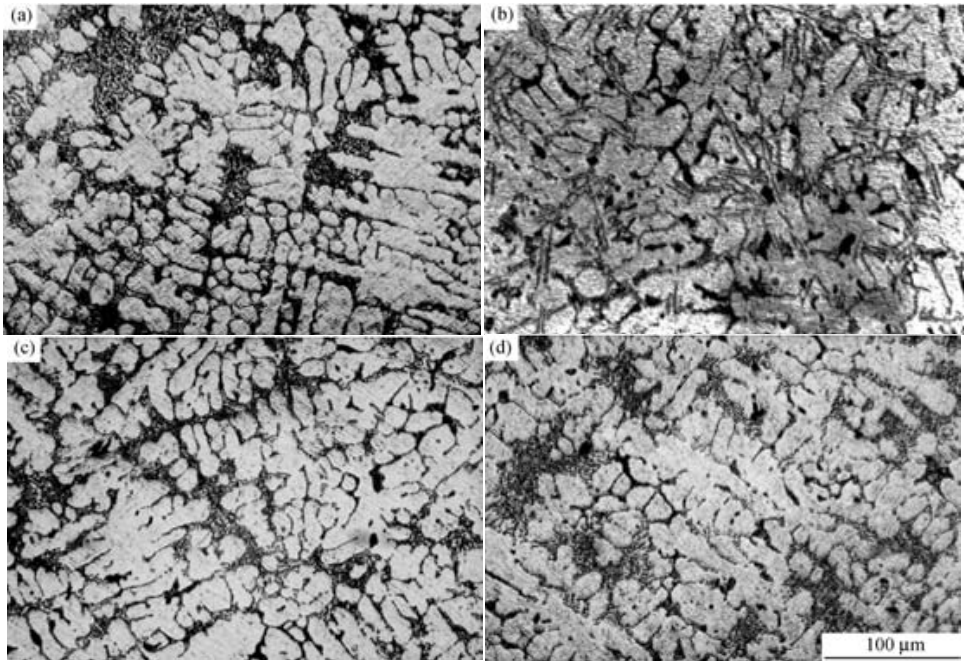

Fig 4.9 Typical microstructures of sodium- or barium-modified commercial ZL107 alloy (0.5%HF): (a) Na, 0.5h; (b) Na, 2 h; (c) Ba, 1 h; (d)Ba, 6 h. [7]

Al–7Si alloy was prepared by melting commercially pure aluminum (99.7% pure) with the Al–20Si master alloy in a graphite crucible in a pit-type resistance furnace at 720 ◦C.

Table 4.1 [7]

Table 1
Grain size and DAS of Al and Al–7Si alloy

Specimen	Addition level of grain refiner (wt.%)	Grain size, μm (for Al)/DAS (for Al–7Si) at different holding times				
		0 min	5 min	30 min	60 min	120 min
Al	0.2% M51	220	110	86	132	145
Al–7Si	0.2% M13	46	–	19	20	22
Al–7Si	0.66% M13	46	–	18	18	18
Al–7Si	1.0% M13	46	–	16	17	17
Al–7Si	1.33% M13	46	–	16	17	17
Al–7Si	2.0% M13	46	–	16	17	17
Al–7Si	1.0% M03	46	–	17	17	17
Al–7Si	1.0% M30	46	–	26	30	34
Al–7Si	3.33% M30	46	–	19	20	21

Al (99.7% pure) was grain refined with Al–5Ti–1B (M51) grain refiner and Al–7Si alloy was grain refined by using Al–1Ti–3B (M13), Al–3Ti (M30), and Al–3B (M03) grain refiners at various holding times (0, 5, 30, 60 and 120 min). Zero minute holding time refers to the sample cast without the addition of grain refiner. It is clear from Table 4.1 that the grain size of Al, grain refined with 0.2 wt.% of M51 master alloy, decreases with increase in holding time from up to 30 min and from 60 to 120 min, the grain size increases slightly. Figure 4.10a and 4.10b shows the microstructures of Al and Al-7Si alloy with refiners.

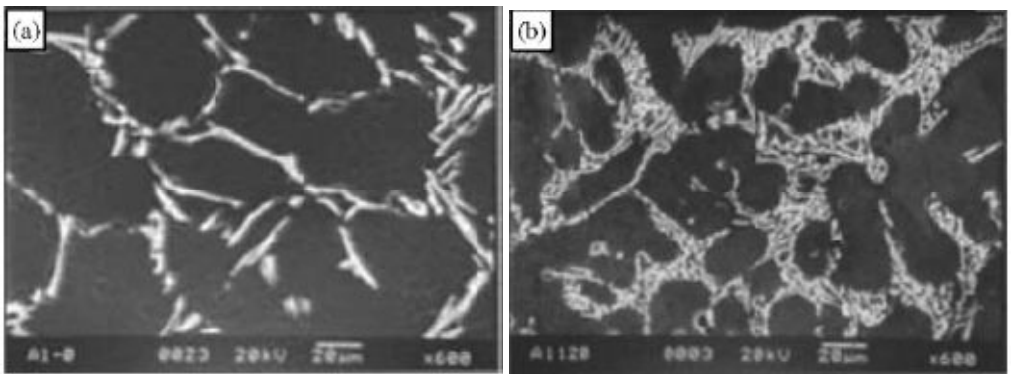

Fig 4.10(a) with out addition of grain refiner and **fig 4.10(b)** with addition of 1.0 wt.% M13 grain refiner (120 min holding time). [7]

4.8 A. Knuutinen et. al. [8] studied the modification of Al–Si alloys with Ba, Ca, Y and Yb. It can be clearly observed in above Figure 4.11 shows that the first addition of Ca, 36 ppm, causes a large change in the cooling curve compared to the unmodified alloy. The corresponding microstructure contains well modified fibrous silicon. Further increases in

calcium content do not seem to alter the cooling curves significantly, i.e. the eutectic growth temperature and recalescence seems largely unaffected, and the eutectic microstructure remains well-modified and does not change significantly with increased calcium content.

4.9 K.G. Basavakumar et. al. [9] have reported the effect on toughness by additions of modifiers and grain refiners. They reported the Sr as a modifier and Ti and B master alloy as a grain refiner. It is observed that grain refinement, modification and combined addition of both refiner and modifier have profound influence on microstructures of the Al–12Si and Al–12Si–3Cu cast alloys.

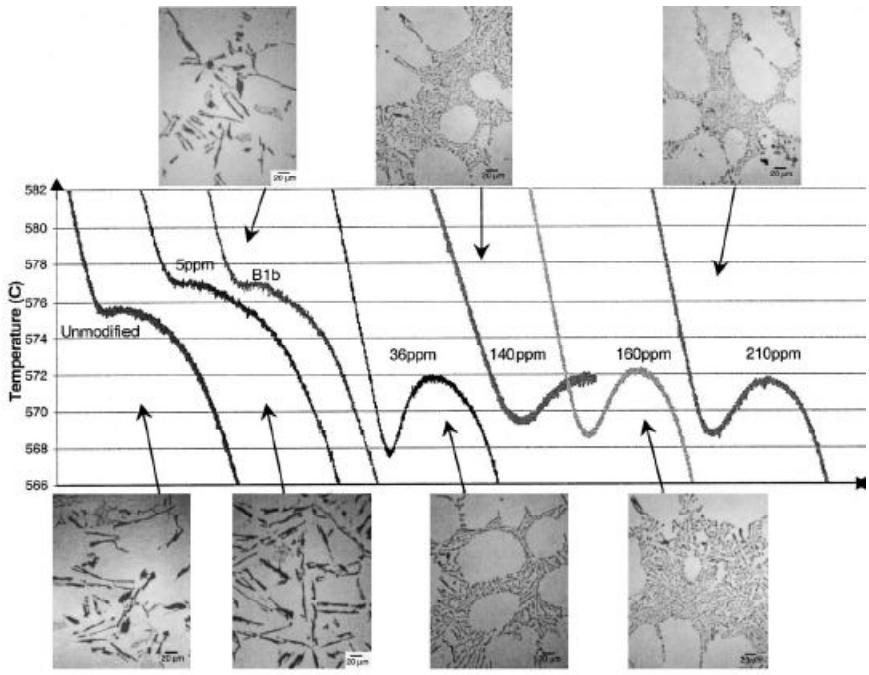

Figure 4.11 Assembly of cooling curves, with focus on the eutectic reaction, for all tested Ca addition levels to the A356.0 alloy with corresponding optical micrographs of representative eutectic structure in each sample. [9]

The results also suggest that the addition of Al–1Ti–3B master alloy along with Sr modifier to Al–12Si and Al–2Si–3Cu cast alloys shows more uniformly distributed α-Al dendrites, fine silicon and $CuAl_2$ particles in the interdendritic region compared to the individual addition of grain refiner or modifier. It is important to note that the alloys have been cast in a graphite mould surrounded by fireclay brick (slow cooling). Thus, further improvement in the

impact toughness can be expected for fast cooled castings, as this can lead to further refinement of the microstructures.

Impact toughness of Al–12Si and Al–12Si-3Cu cast alloys mainly depends on the shape, type, size and size distribution of α-Al grains, silicon particles and $CuAl_2$ phases in the matrix. The measurements performed confirmed that the impact properties are mainly influenced by the sizes of the soft phase and eutectic constituents in the alloys. The increase in impact toughness consists of two parts: the breakage of the large aluminum dendrites into more uniformly distributed α-Al dendrites by refinement and the plate-like eutectic silicon to fine broken particles of silicon and massive blocks of $CuAl_2$ to fine micro constituents of $CuAl_2$ by modification. The combined addition of grain refiner and modifier (Al–1Ti–3B+Sr) to Al–12Si–3Cu alloy shows remarkably improved impact toughness (8.7370.1 J/cm2) when compared to untreated Al–12Si alloy (1.6370.5 J/cm2).

4.10 N. Saheb et. al [10]. reported the addition of Ti content in the Al/Si alloys and their hardness behavior with increment of Ti content.

According to author Figure 4.13 shows the microstructure of the as-cast A1-12 wt% Si alloys with various Ti contents (alloys A). Figure 4.13*(a)* reveals the microstructure of the binary Al-Si alloy Al, which consists of a-A1 phase and eutectic and table 4.2 shows the different composition of Al/Si with Ti content are used.

Table 4.2 composition of Ti in Al/Si alloy [10]

	Composition (wt%)		
Alloy	Al	Si	Ti
A1	Balance	11.55	0.00
A2	Balance	11.93	1.05
A3	Balance	11.78	1.70
A4	Balance	11.75	2.15
A5	Balance	11.98	2.88
A6	Balance	11.46	3.96

As can be seen in the micrographs shown in figures 4.13*(b-f)* for alloys A2-A6 respectively, the addition of Ti led to the precipitation of a new phase. From the microstructural, phase and chemical characterizations, one may deduce that in the Al-rich corner of the Al-Si-Ti system, for low Si contents (probably lower than the binary eutectic value of 12.5 wt%Si), only the phases *α*-Al, Si and A1,Ti of the binary systems Al-Si and Al-Ti are present. Figure shows

the increase in the hardness value with increasing the Ti content in the Al/Si alloy this effect is due to the age hardening effect of the Al_3Ti phase. The Vickers microhardness changes of alloys heat treated at 200 and 400°C are given in figure for alloys Al, A4 and A6.

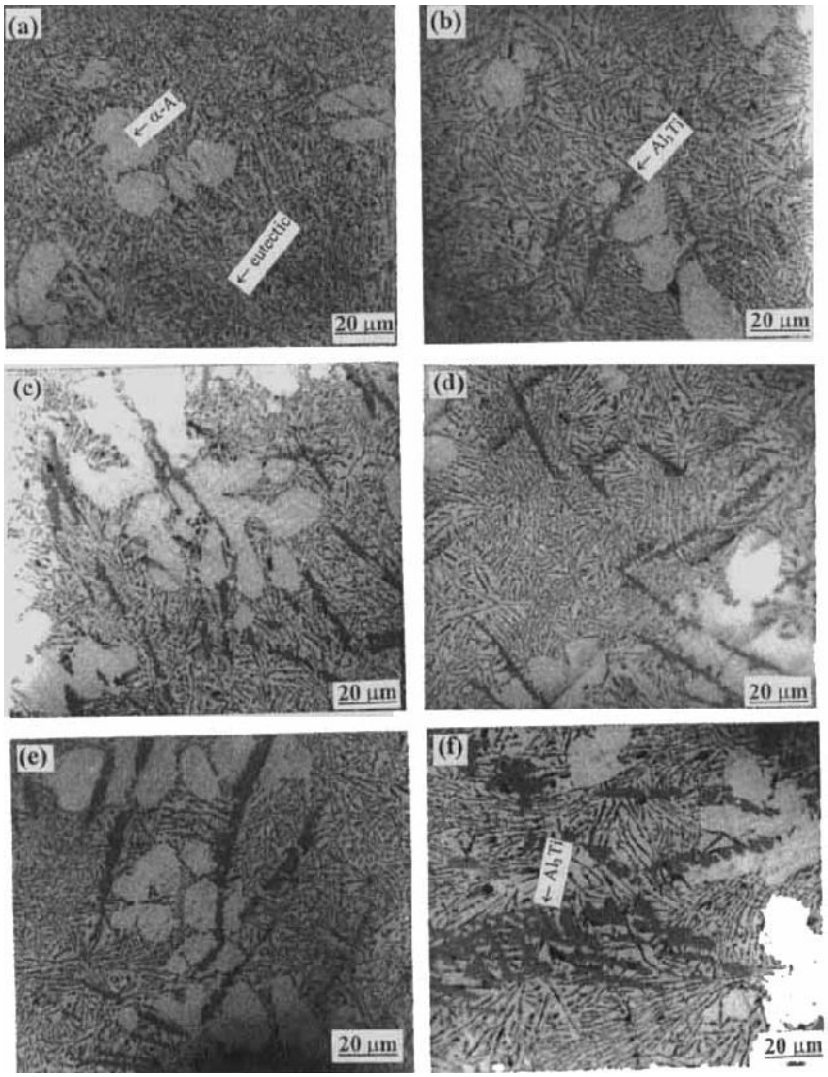

Figure 4.13 Microstructures of the as-cast alloys: ***(a)*** alloy **Al; *(b)*** alloy **A2; *(c)*** alloy **A3;*(d)***alloy **A4; *(e)*** alloy **A5; (f)** alloy **A6. [10]**

Alloys heat treated at 200°C showed some response to age hardening and the microhardness increased slightly as shown in figures below the possibility of clustering of Si particles, ageing at 200°C may lead to the precipitation of fine particles of intermetallic compound A13Ti in alloys A2-A6. These fine precipitates will contribute to an increase in the microhardness. The addition of Ti to Al-12 wt% Si alloy results in the precipitation of the

intermetallic compound A1-Ti which dissolves up to 13.12at.% **Si** The microhardness of both as-cast alloys

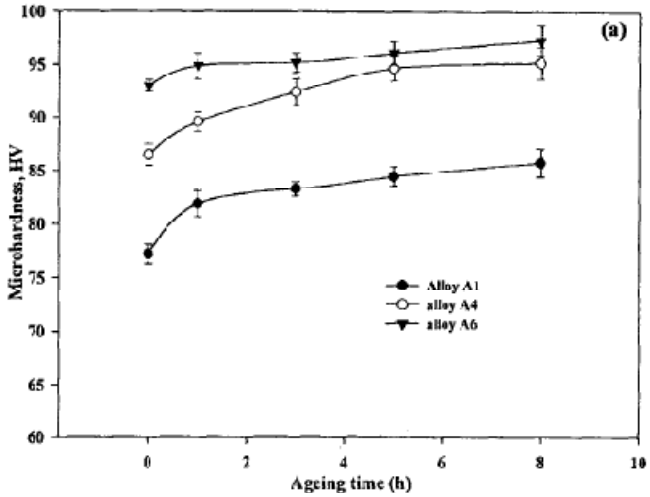

Fig 4.14 Aging behavior of Ti-containing AI-Si [10]

increased with increasing Ti content as a result of the precipitated phases fig 4.14. Ageing at 200°C seems to induce the diffusion of Si and Ti, leading to clustering of Si particles and precipitation of fine particles of A1, Ti which contribute to the increase in the microhardness of the Ti-added alloys

4.11 Dheerendra Kumar Dwivedi et. al. [11] have reported the influence of silicon particle morphology on mechanical properties of two piston alloys has been reported. Alloys having nominal composition Al-12%Si-1%Ni-0.8%Cu-0.6%Mg (LM13) was prepared by melting and casting.

The eutectic silicon crystals are plate like in appearance (Fig 4.14a). Melt treatment affects the microstructure of LM13. Grain refinement reduces the interdendritic arm spacing of α-aluminium dendrites. Dendrite arm spacing is reduced from 50 to 25 μm due to grain refinement Fig 4.15b. Modification refines eutectic silicon crystals and changes the morphology of these crystals from acicular to fibrous. Finer structure is observed in Fig 4.15b rather than in Fig 4.15a. Heat treatment of LM13 results in significant change in morphology of eutectic silicon and aluminum grains. Heat treatment causes spheroidization of eutectic silicon crystals (Fig 4.15c). It may be observed that spheroidization of silicon crystals takes place predominantly in the vicinity of grain boundaries.

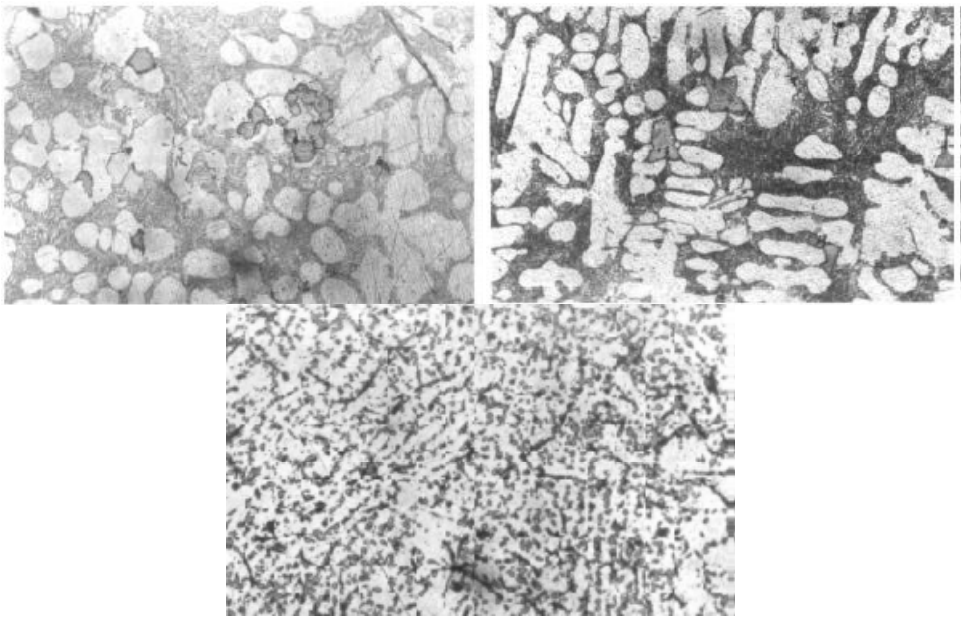

Figure 4.15 Microphotographs of LM13 under a) as-cast, b) melt-treated, and c) heat-treated conditions (200X). [11]

As-cast alloy (Fig 4.15a) is already modified to some extent because of high cooling rate (due to casting in a metallic mold). However, the shape of eutectic silicon is still acicular/needle type. It may be attributed to a higher growth rate of the aluminum phase than the silicon because of low latent heat and high thermal conductivity of the former compared with the latter. Due to the high growth rate of aluminum, it forms a cover/envelop around the silicon crystal and prevents its growth.

Table 4.3 [11]

Alloy Condition	As Cast	Melt Treated	Heat Treated
Tensile Strenth(N/mm^2)	205	224	252
Hardness(VHN)	102	110	124
Ductility(% Elongation)	1.5	1.8	2.5

Needle-shape morphology of silicon crystals is not favorable from a mechanical property point of view because such silicon crystals act as internal stress raisers and provide easy paths for fracture. Silicon precipitates mainly in the form of needles within the Al–Si eutectic along with a dispersed Mg_2Si phase. Modification of the alloy by strontium produces the fine

eutectic of Al-Si, and the morphology of eutectic silicon changes from needle/acicular to fibrous (Fig 4.15b).

The addition of strontium may lower the nucleation as well as the growth temperature during solidification. These two factors would increase the nucleation rate and decrease the growth rate. A fine, intimate mixture of aluminum and silicon is formed due to modification. It may also be attributed to the fact that strontium reduces the surface tension of liquid aluminum, which prevents the growth of eutectic silicon crystals. Refinement of α-aluminum dendrites with the addition of Al-5%Ti-1%B grain refiner in the molten alloy takes place due to the fact that nuclei such as TiB_2 and $TiAl_3$ are produced in the melt. These particles provide many nucleation sites, which ultimately leads to fine-grained structure of aluminum. Eutectic silicon particles are spheroidized in the matrix of aluminum after heat treatment (Fig 4.15c). This morphology can reduce the stress concentration at particle-matrix interfaces and discourage the nucleation of cracks and their propagation under external load. Hence, spheroidization of silicon crystals can be attributed to an increase in tensile strength and ductility after heat treatment. Heat treatment of the alloy causes complete dissolution of Mg_2Si, and the entire network of silicon is broken down into fine globules.

Modification of LM13 using strontium refines the eutectic silicon crystals, and simultaneously, the addition of Al-5%Ti-1%B reduces the dendrite arm spacing of aluminum grains. This refinement of aluminum dendrites and eutectic silicon enhances tensile strength and ductility. Refinement of primary silicon particles using red phosphorous also enhances the mechanical properties.

4.12 K T KASHYAP et. al. [12] have reported the Effects and mechanisms of grain refinement in aluminum alloys. Grain refinement plays a crucial role in improving characteristics and properties of cast and wrought aluminum alloys. Generally Al–Ti and Al–Ti–B master alloys are added to the aluminum alloys to grain refine the solidified product.

Figure 4.16 shows the microstructure of 356 alloys after grain refinement with Al–5Ti–1B master alloy. Note the fine dendrite arm spacing of the solidified structure. The segregating power of an element is described by **growth restricting factor (GRF)** during solidification. The GRF is a measure of the growth restricting effect of solute elements on the growth of solid–liquid interface of the new grains as they grow into the melt.

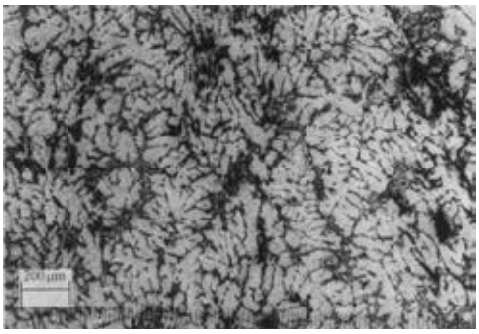

Figure 4.16 Microstructure of Al–Si (356) alloy
after grain refining with Al–5Ti–1B master alloy (50X). [12]

Table 4.4 Typical values of these parameters for common alloying elements [12]

Element	k_i	m_i	$(k_i - 1)m$	Maximum concentration (wt%)	Reaction type
Ti	~ 9·0	30·7	245·6	15·00	Peritectic
Ta	2·5	70·0	105·0	~ 0·10	Peritectic
V	4·0	10·0	30·0	~ 0·10	Peritectic
Hf	2·4	8·0	11·2	~ 0·50	Peritectic
Mo	2·5	5·0	7·5	0·10	Peritectic
Zr	2·5	4·5	6·5	~ 0·11	Peritectic
Nb	1·5	13·3	6·6	~ 0·15	Peritectic
Si	0·11	– 6·6	5·9	~ 12·60	Eutectic
Cr	2·0	3·5	3·5	~ 0·40	Peritectic
Ni	0·007	– 3·3	3·3	~ 6·00	Eutectic
Mg	0·51	– 6·2	3·0	~ 3·40	Eutectic
Fe	0·02	– 3·0	2·9	~ 1·80	Eutectic
Cu	0·17	– 3·4	2·8	33·20	Eutectic
Mn	0·94	– 1·6	0·1	1·90	Eutectic

It is defined as $mC_0(k - 1)$, where m is the liquidus gradient, C_0 the bulk composition, k the partition coefficient between solid and liquid. Typical values of these parameters for common alloying elements are presented in table 4.4.

When a number of solutes are present in the melt, the GRFs are added which assumes that there is no interaction between solutes.

$$\mathbf{GRF} = \boldsymbol{m_i(k_i - 1)C_0}$$

The criterion for constitutional super cooling is

$$\frac{G_L}{R} \geq \frac{-\sum m_i C_0 (1 - k_i)}{kD_L}$$

We can see that the growth rate is inversely proportional to $m_i C_0 (k_i - 1)$. Li *et al* (1997) have suggested that the reason for grain refinement caused by titanium additions is due to the titanium as a solute. They suggest that the powerful segregating ability of titanium as solute leads to a constitutionally under cooled zone in front of the growing interface within which nucleation can occur on nucleates that are present. Cast alloys are more difficult to grain refine than wrought alloys. The reason for this is thought to be the high level of alloying elements particularly silicon. Al–Ti–B grain refiners with excess titanium have been found to be poor grain refiners. Al–4%B master alloy is a much effective grain refiner than Al–6%Ti or Al–8 %Ti– %B in casting alloys. Al–Si alloy solidify with a eutectic structure with lamellae of *a*-Al and eutectic silicon. Na, Sr are added to the alloy during casting to alter the morphology of the lamellar eutectic silicon to spheroidal form. This is termed as modification. Modification generally improves mechanical properties like ductility and fracture toughness. When a grain refiner is added to the alloy, there is a critical holding time where the grain size is minimum. Beyond the critical holding time, grain size of the casting increases. This effect is known as 'fade'. Sigworth and Guzowski (1985) developed an Al–3%Ti–3%B alloy where (Al, Ti)B_2 crystals are the nucleant particles present for grain refinement of casting alloys. They found that AlB_2 crystals in Al–B master alloy dissolve and the fade time to be short. Further they found it to poison Sr modification whereas Al–3Ti–3B master alloy provides consistent grain refining with little fade and does not poison strontium modification.

4.13 Shufang Yao et. al. [13] have reported the application of CX-type modifiers in Al-Si alloys.

The CX-type **(CX means the modifiers that have long effective term)** modifiers which were studied in recent years are a new type modifiers of Al-Si alloys [3,4]. They have overcome the defects of traditional modifiers. Table 4.5 and Figure 4.17(a & b) shows the results of microstructures and mechanical properties of ZL108 Al-Si alloy which was treated melting ZL108 alloy was kept for 8 h after the modifiers were added into the molten alloy.

It is shown that the modification effects of CX-type modifier are better than that of the red phosphorous powder. In addition, the red phosphorous powder and the Na-salts were used as the modifiers of ZL108 alloy and ZL104 alloy for comparing experiments respectively. The amount of the addition of red phosphorous is 0.1% to ZL108 alloy, and the amount of the addition of Na-salts modifier is 1.4%-2.0% to ZL104 alloy. The effects (such as the microstructure, the mechanical properties of alloys, the service properties of castings

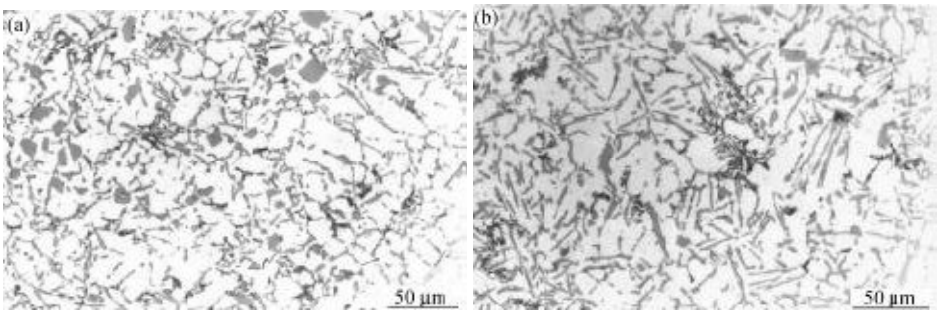

Figure 4.17 Microstructure of ZL108 Al-Si alloy modified with CX-type modifier and red phosphorous powder respectively**, (a)** modified with CX-01 modifier; **(b)** modified with red phosphorous powder.[13]

Table 4.5 shows the results under the same conditions as above; in addition, in maintained time the melting alloy was kept for 8 h.

Table 4.5 maintained time the melting alloy was kept for 8 h [13]

Modifier	Addition / %	Primary Si size / μm	Eutectic Si size / μm	σ_b / MPa	$\sigma_{b,(300℃)}$ / MPa	HB
CX-01	0.1	<40	<60	355-360	≥104	121
Red P	0.1	100-120	100-120	340-350	≥80	121

and the technical economical benefit *etc.*) of CX-type modifiers were synthetically evaluated with the national standards: GB10849-89 (The Modification of Cast Al-Si Alloys), GB1173-86 (Cast Al Alloys), JB3931-85 (The technical requirement of piston used in automobile engine and motor engine), and the standard (JB3932-85) which is related to metallography. The CX-type modifiers have double modification functions. They can simultaneously refine the primary silicon and modify the eutectic silicon in Al-Si alloys. They can improve the morphologies of the primary silicon and the eutectic silicon in Al-Si alloys. Therefore, they increase the mechanical properties such as tensile strength and elongation of Al-Si alloys. The amount of the addition of CX-type modifiers is small. Their modification effects can act quickly and can last up to 8 h. Their modification results are better than most other kinds of modifiers of Al-Si alloys. The operations of CX-type modifiers are simple. There is no smoke, no irritant or awful smell in the modifying process of using CX-type modifiers. They do not have the problem of environment pollution. CX-type modifiers are of advanced level in both technology and economy. They are used quite well by some companies.

4.14 H. Liao et. al. [14] reported the Influence of boron on the microstructure and mechanical properties of Al –11.6Si – 0.4Mg casting alloy modified with strontium. Al – 1B master alloy has a strong action in refining the dendritic structure in near eutectic Al – Si casting alloys modified with Sr. The SrB combined melt treatment can improve considerably the mechanical properties of the alloys, both as cast and after T6 heat treatment. The addition of strontium to the Al – 11.6%Si – 0.4%Mg alloy promotes the growth of columnar dendrite. The slender columnar dendrites are arrayed as groups with a specific growth orientation, as shown in Fig. 4.18*a*.

Table 4.6 presence of Sr and B content in the samples [14]

Sample number	1	2	3	4	5	6	7
Sr content, wt %	...	0·030	0·030	0·030	0·030	0·030	0·030
B content, wt %	...	...	0·012	0·020	0·028	0·036	0·044

Figure 4.18(*a–f)* shows the change in shape and size of the dendritic a phase with varying B content in Al – 11.6%Si– 0.4%Mg alloys modified with 0.030%Sr. The addition of 0.012%B

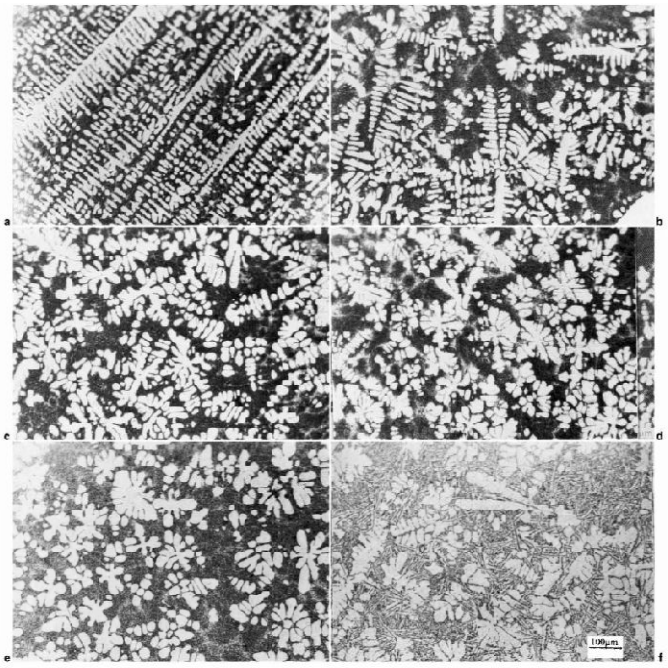

Fig 4.18- a 0%B; **b** 0.012%B; **c** 0.020%B; **d** 0.028%B; **e** 0.036%B; **f** 0.044%B Morphology and size of dendritic a phase with varying B content in Al – 11.6%Si – 0.4%Mg–0.030%Sr alloys. [14]

results in a remarkable decrease in the size of the dendrites and a considerable change of the shape. Majority of the equaixed dendrites without any specimen growth orientation, and a small quantity of the columnar dendrites with remarkably shortened size.

These results show that Al – 1B master alloy gives strong refinement of the dendritic a phase in near eutectic Al – Si alloys modified with Sr. A level of 0.044%B causes the shape of the dendrites to degenerate, with Dendrite II appearing again in the microstructure, as seen in Fig 4.18*f*; the size of the dendrites is increased considerably and the shape becomes less rounded. This indicates that refinement of the dendrite has been poisoned by too great a boron addition. Fig 4.18f also shows that the eutectic silicon phase changes again into coarse flakes. In other words, the modification by strontium of the eutectic silicon is also poisoned.

4.15 M. A. MOUSTAFA and et. al. [15] reported the effect of solution heat treatment and additives on the hardness, tensile properties and fracture behavior of Al-Si (A413.1) automotive alloys.

The alloys listed in Table 4.6 are grouped into three categories to facilitate discussion of the results:(i) the base A413.1 alloy, M0, (ii) alloys M1 through M3N, with M1 (viz., Sr-modified M0 alloy) representing the base or reference alloy for this group, and (iii) alloys M4 through ZN, having M4 as their reference alloy.

Table 4.6 [15]

	Chemical composition (wt%)												
Alloy code	Si	Fe	Cu	Mn	Mg	Cr	Ni	Zn	B	Be	Sr	Ag	Ti
M0[a]	11.90	.88	.875	.210	.082	.017	.017	.340	.008	.000	.002	.000	052
M1[b]	11.74	.793	.875	.211	.086	.026	.020	.338	.008	.000	.030	.000	051
M2	11.79	.789	.867	.206	.411	.018	.019	.343	.007	.000	.026	.000	050
M2N	11.46	.749	.878	.199	.422	.017	.023	.334	.007	.000	.000	.000	050
M2E	11.72	.761	.867	.196	.446	.018	.024	.324	.007	.018	.025	.000	051
M3	11.74	.800	2.64	.193	.070	.040	.022	.321	.008	.000	.039	.000	051
M3N	11.76	.798	2.66	.195	.067	.040	.022	.331	.008	.000	.000	.000	051
M4[c]	11.28	.751	2.61	.184	.379	.033	.027	.313	.007	.000	.041	.000	052
M4N	11.28	.751	2.61	.184	.379	.033	.027	.313	.007	.000	.000	.000	052
A	11.65	.722	2.70	.182	.366	.016	.030	.031	.009	.000	.025	.715	050
AB	11.48	.720	2.73	.182	.396	.017	.032	.309	.009	.016	.034	.710	050
1NN	11.86	.678	2.46	.200	.314	.018	.627	.241	.002	.000	.000	.000	050
1N	11.86	.678	2.46	.200	.314	.018	.627	.241	.002	.000	.021	.000	050
2N	11.88	.673	2.43	.192	.378	.020	1.41	.240	.002	.000	.026	.000	050
Z	11.95	.706	2.81	.198	.378	.019	.029	2.74	.002	.000	.020	.000	046
ZN	11.89	.677	2.66	.192	.444	.019	.634	2.25	.002	.000	.021	.000	053

Addition of Sr decreases the hardness and strength (YS, UTS) of the Mg-containing alloys, which could probably arise from a retardation of the precipitation of Mg_2Si during the aging

process (i.e., increasing the incubation period prior to the commencement of precipitation), regardless of the solution time at 500^{o}C. Transmission electron microscopic examination is required to confirm this suggestion. The copper-containing alloys, however, are less sensitive to the presence of Sr.

All alloying element additions, i.e., Mg, Cu, Be, Ag, and Zn result in improving the hardness and strength of the base alloy, especially in the T6 condition. Addition of Ni (up to 1.41%), however, decreases the hardness and tensile properties (YS, UTS and %Elongation) of the alloy. This may be interpreted in terms of the formation of intermetallics which may control the grain size, rather than contribute to the hardening of the heat treated alloys. In unmodified alloys, cracks initiate within the brittle acicular Si particles themselves, without passing through the ductile Al matrix, whereas in modified alloys, the cracks propagate through interdendritic regions, leading to the deformation of the α-Al dendrites, their pinpoint shapes indicating their ductile nature. The number of cracked Si and intermetallic particles beneath the fracture surface increases with the increase in the ultimate tensile strength of the alloy. The latter is a function of the type and amount of alloying elements added.

4.16 H.S. Kang et. al. [16] have reported the effective parameter for the selection of modifying agent for Al–Si alloy.

The base alloy of the Al–14 wt.% Si alloys was prepared using pure Al (bulk type, 99.99%) and Si (lump type, 99.9999%) by induction melting under an argon environment. Sr, Y, Sm and Gd were selected as modifying elements and prepared as master alloys (Al–9Sr, Al–87Y, Al–7Sm and Al–6Gd). Starting with binary Al–14 wt.% Si, 0.1–3 wt.% of a modifying agent was added to the base alloy to investigate the effect of the modifying agent. The mixture of alloys was remelted in a graphite crucible by induction melting under an argon environment and poured into a preheated graphite mold to prevent rapid solidification. The microstructures of each specimen were observed using optical microscopy(OM) and scanning electron microscopy(SEM).

As represented in Table 4.7 Sr, Ba and Ca, which were reported to have such a modification effect, not only have similar crystal structures and lattice constants to those of Si, but also have large negative mixing enthalpies with Si. On the other hand, alloying elements such as Cu and Mg, which were reported not to have any modification effect, not only have different crystal structures and lattice constants with Si, but also have small negative mixing enthalpies with Si.

Table 4.7 shows the properties of alloying elements [16]

Element	Group	Crystal structure	Lattice constant (pm)	R/R_{Si}	$\overline{\Delta H}^{\circ}_{X \text{ in Si (interface)}}$	Modification
Si	4B	Cubic	543	–	–	–
Sr	2A	CCP	608.5	1.68	−156	O
Ca	2A	CCP	559	1.85	−154	O
Ba	2A	BCC	502.8	1.85	−164	O
Cu	Transition	CCP	361.5	1.09	−3	X
Mg	2A	HCP	329	1.37	−54	X
Y	3A	HCP	364.7	1.54	−275	
Gd	Rare-earth	HCP	363.6	1.54	−197	
Sm	Rare-earth	Trigonal	362.1	1.29	−193	

Though Y, Sm and Gd have different crystal structures, lattice parameters and atomic radii smaller than 1.65. They were selected to test the new parameter of large negative mixing enthalpies with Si. To investigate the effect of these elements on the microstructure of Al– Si alloy, they were added in the Al–14 wt.% Si alloy. Fig 4.19 shows the unmodified microstructures of the Al–14 wt.% Si alloy in the unmodified state. Fig 4.20(a-d) shows the modified microstructures of the Al–14 wt.% Si alloy with the addition of several modifying agents.

It was well known that Sr had a good modifying ability for eutectic Si crystals. As represented in Fig 4.20a, the eutectic Si crystals were fully modified with the addition of 0.015 wt.% Sr. As represented in Fig 4.20(b and c), with the addition of 3 wt.% Y and 2 wt.% Sm, Which had large negative mixing enthalpy with Si, the eutectic Si crystals were also modified. With the addition of 2 wt.% Gd, the eutectic Si crystals were only refined. With these results of the modified microstructures, it was confirmed that elements selected by mixing enthalpies with Si, such as Y, Sm and Gd, have modification effect. To investigate the reason for the modification of the eutectic Si crystals with elements having large negative mixing enthalpies, the eutectic depression of each modified alloy was measured.

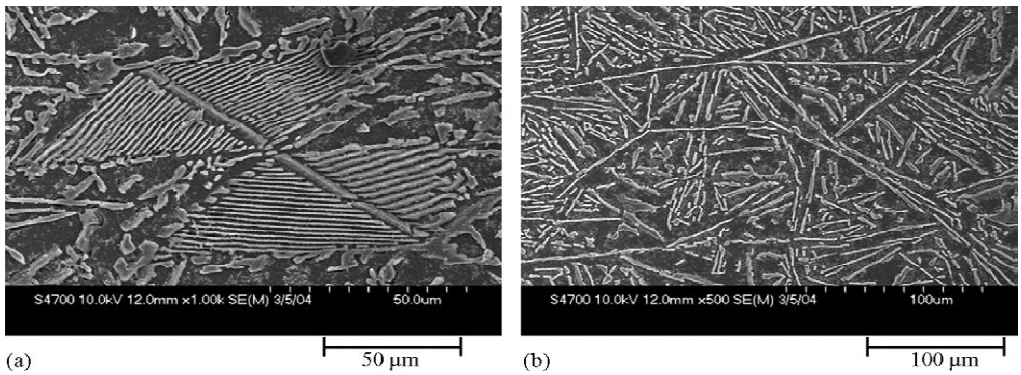

Fig 4.19 Unmodified microstructures of Al–14 wt.% Si: **(a)** primary Si 50_m and **(b)** eutectic Si 100µm. [16]

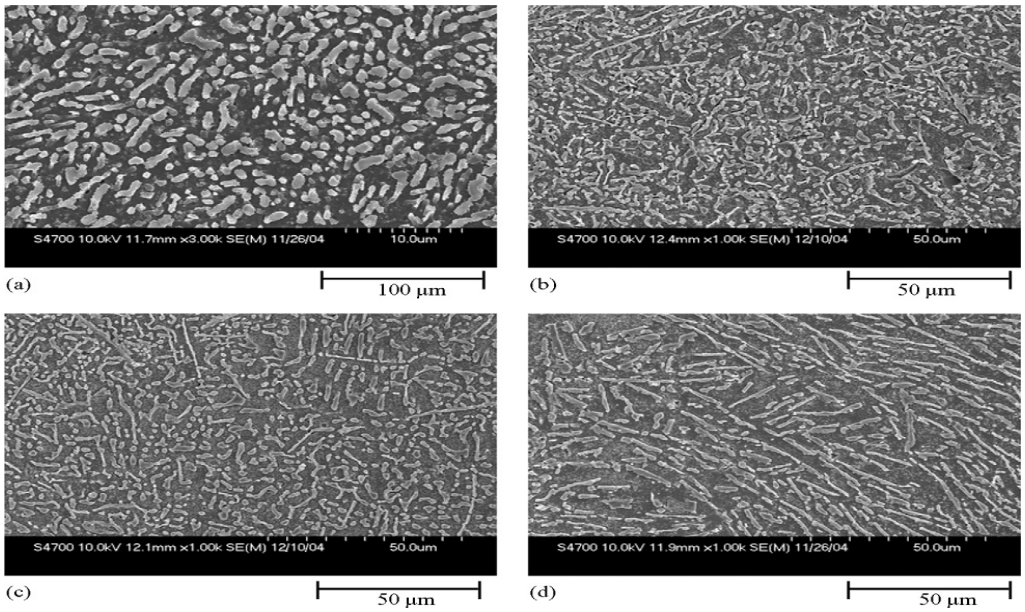

Fig 4.20 Modified microstructures of Al–14 wt.% Si: **(a)** 0.015 wt.% Sr added, **(b)** 2 wt.% Y added, **(c)** 2 wt.% Sm added and **(d)** 2 wt.% Gd added [16]

The large negative mixing enthalpy means strong affinity between two elements and often drops melting. Based on these results, it was concluded that if the eutectic Si crystals nucleate and grow at the temperature sufficiently lower than the eutectic temperature of Al–Si alloy by the addition of an element whose mixing enthalpy with Si is large negative, the growth kinetics of the eutectic Si crystal changes and finally, eutectic crystals are modified.

To select an effective modifying agent for Al–Si alloys, the mixing enthalpy, which was calculated by the Miedema model, was newly considered. Based on the results of our calculations, Y, Sm and Gd that have large negative mixing enthalpies with Si, were tested as modifying agent. It was confirmed that these elements have the modification effect on the eutectic Si crystals and each modified alloy has the value of a eutectic depression larger than 6K. Thus, in addition to crystal structure and lattice parameter, large negative mixing enthalpy with Si is expected to be additional effective parameter for the selection of a modifying agent for Al–Si alloys and it is concluded that the reason for the modification of eutectic Si crystals is the eutectic depression which results from the addition of the modifying agent.

CHAPTER – 5

EXPERIMENTAL

In this chapter all the details about the preparation and characterization of samples has been described. In the present work, the casting technique has been utilized to prepare the samples of aluminum alloys. The experimental technique involves following steps:

- Casting
- Preparation of samples
- Characterization and Testing

The alloy composition that is selected for present study is:

5.1 Composition Used

Table 5.1 shows the composition of element used in the casting of samples.

Table 5.1 composition of element used in the casting of samples

Elements	Al (wt%)	Al-Si Master Alloy (wt%)	Bi (wt%)	Ca (wt%)	Sn (wt%)	Pb (wt%)	Cd (wt%)
Sample-1	64	41.4	--	--	--	--	--
Sample-2	64	41.4	4.5	--	--	--	--
Sample-3	64	41.4	--	4.5	--	--	--
Sample-4	64	41.4	--	--	4.5	--	--
Sample-5	64	41.4	--	--	--	4.5	--
Sample-6	64	41.4	--	--	--	--	4.5
Sample-7	64	41.4	4.5	4.5	--	--	--
Sample-8	64	41.4	4.5	--	4.5	--	--
Sample-9	64	41.4	4.5	--	--	4.5	--
Sample-10	64	41.4	4.5	--	--	--	4.5
Sample-11	64	41.4	--	4.5	4.5	--	--

Sample-12	64	41.4	--	4.5	--	4.5	--
Sample-13	64	41.4	--	4.5	--	--	4.5
Sample-14	64	41.4	--	--	4.5	4.5	--
Sample-15	64	41.4	--	--	4.5	--	4.5
Sample-16	64	41.4	--	--	--	4.5	4.5
Sample-17	64	41.4	4.5	4.5	4.5	--	--
Sample-18	64	41.4	4.5	4.5	--	4.5	--
Sample-19	64	41.4	4.5	4.5	--	--	4.5
Sample-20	64	41.4	4.5	--	4.5	4.5	--
Sample-21	64	41.4	4.5	--	4.5	--	4.5
Sample-22	64	41.4	4.5	--	--	4.5	4.5
Sample-23	64	41.4	--	4.5	4.5	4.5	--
Sample-24	64	41.4	--	4.5	4.5	--	4.5
Sample-25	64	41.4	--	4.5	--	4.5	4.5
Sample-26	64	41.4	--	--	4.5	4.5	4.5
Sample-27	64	41.4	4.5	4.5	4.5	4.5	--
Sample-28	64	41.4	--	4.5	4.5	4.5	4.5
Sample-29	64	41.4	4.5	--	4.5	4.5	4.5
Sample-30	64	41.4	4.5	4.5	--	4.5	4.5
Sample-31	64	41.4	4.5	4.5	4.5	--	4.5
Sample-32	64	41.4	4.5	4.5	4.5	4.5	4.5

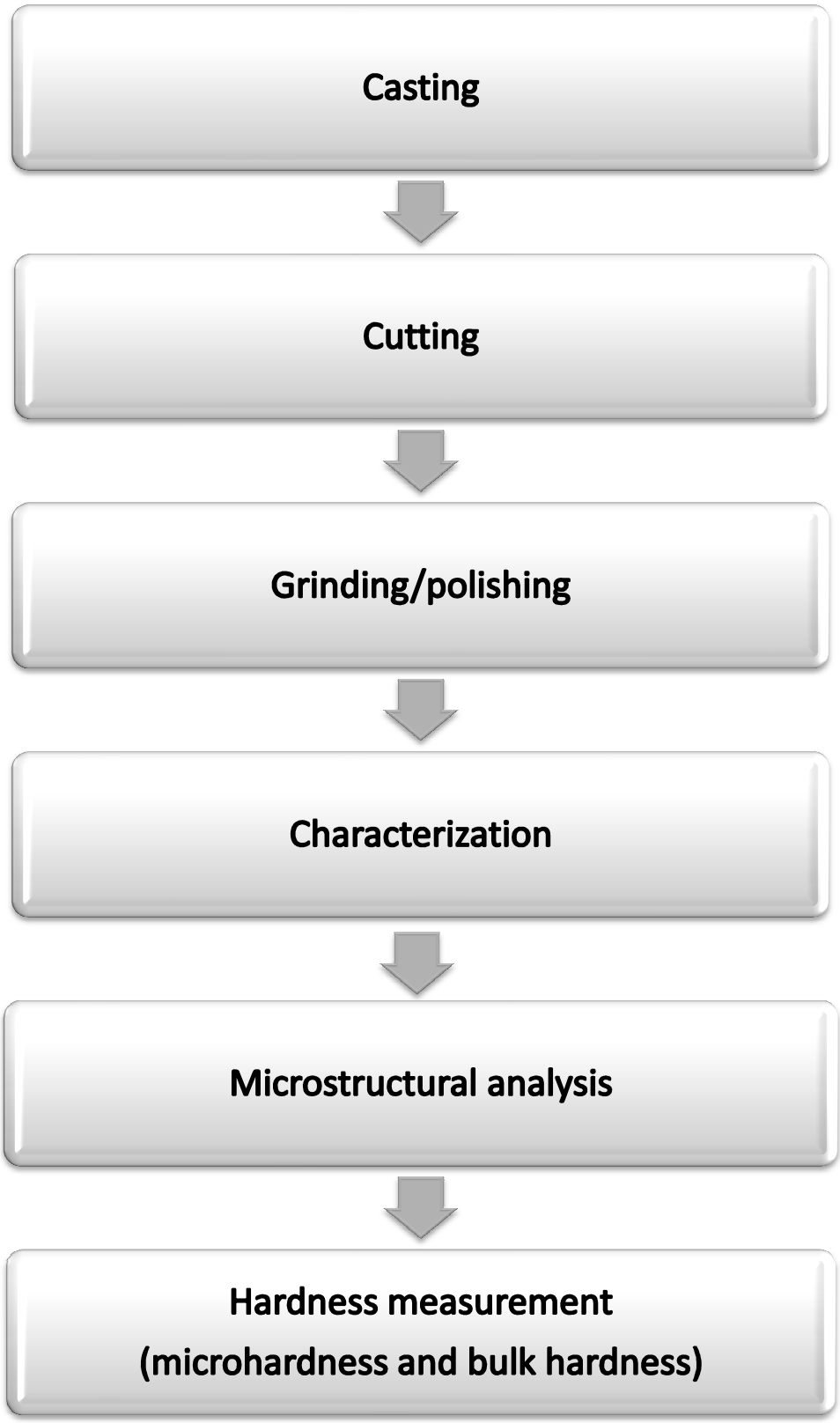

Figure 5.1 – showing flow chart of the process

5.2 Preparation of Al-Si Master alloy

Al-Si master alloy had been prepared to retain the same composition of silicon and to reduce the amount of slag formation in each cast sample. In the preparation of master alloy following materials with given purity grades had been used.

Aluminum- 99.9%

Silicon- 99.9%

Two plates of the master alloy had been prepared (fig 5.2). Total weight of the master alloy after preparation was 1160gm. Some loss of the weight had been observed in the master alloy due to the formation of the slag during melting of the sample.

5.3 Chemical composition test

Chemical composition test had been done (fig 5.3) to know the percentage of silicon in the Al-Si master alloy leads to following result.

1. For plate number 1 the chemical composition of silicon is - 31%
2. For plate number 2 the chemical composition of silicon is - 32%

As a result the average chemical composition of the silicon in the master alloy comes out to be 31.5%. This chemical composition of master alloy is used to prepare eutectic Al-Si alloy for each sample.

5.4 Purity grades of materials

Following grades of materials had been used for casting. Bismuth, Calcium, Tin, Lead, Cadmium were in granular form and silicon is in flakes form.

- Aluminum -- 99.9%
- Silicon – 99.9%
- Bismuth – 99.5%
- Calcium – 99.5%
- Tin – 99.5%
- Lead – 99.5%
- Cadmium – 99.5%

5.5 Casting

Equivalent quantities of the various metals granular were taken by weight. For making each 105.4gm batch, the weighing was done in a very accurate weighing balance (Sigma).

Fig 5.2 Master alloy sample

Fig 5.3 Showing chemical composition testing of master alloy

Sample 1 (Al- 12.6%Si) the quantities of the metals taken as:

Al = 64gm

Al/Si master alloy = 41.4gm

For each sample after weighing metal granular, they are put into the fire-clay crucible. Then the crucible with metal charge is placed into the furnace which is heated up to 750°C and metal is allowed to melt. Stirring is done while melting and complete mixing of charge. When all the granular melt and mixed completely, the molten metal is removed from the furnace and poured into an iron mould. After allowing the metal to cool and solidify in the shape of the mould, the casted samples are taken out of mould. Similarly total 32 numbers of sample had been prepared with different composition given in table 5.1.

5.6 Sample preparation

5.6.1 Cutting

The cast samples are cut in the transverse direction with the help of hexa in the four equal parts. The one of the piece of the cut sample is used for sample preparation (fig 5.4 & 5.5).

5.6.2 Grinding/polishing

The cut samples prepared above had an uneven surface. So the cut samples were then taken

Figure 5.4 showing sample

Figure 5.5 showing sample cut into four pieces

for grinding/polishing operation. The sample was first held over a grinding machine with a moving belt to obtain a smooth surface. The grinding was done in such a way so that all the scratches are in the same direction and the grinded surface becomes flat. After this the samples were polished properly using different grits of emery papers. Because the samples being aluminum alloy, aluminum being soft, it is rubbed over the 200 and 320 grit emery paper for a small time. Then it was rubbed over an emery paper of 400 grit and then over a very fine emery paper of 600 grit for a considerable time in order to get a smooth and clear surface of the sample (fig 5.6).

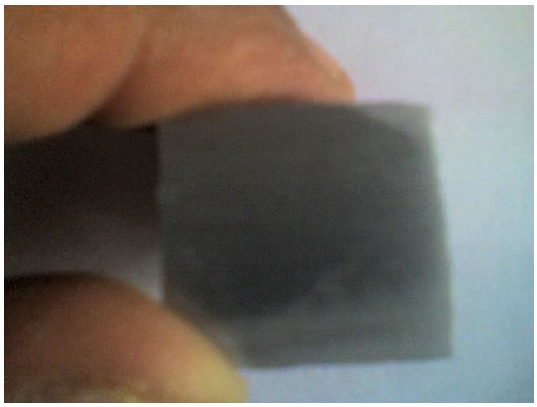

Figure 5.6 showing grinded sample

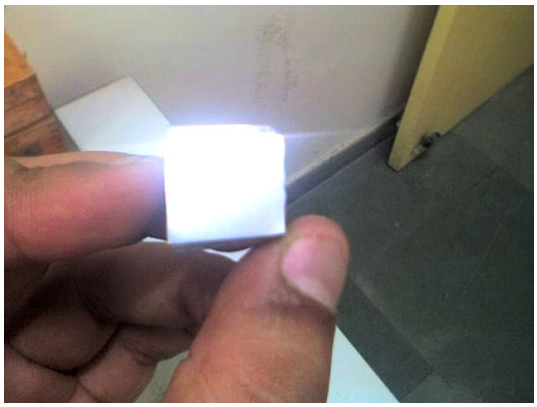

Figure 5.7 showing polished sample

The sample was then polished on a fine polishing machine using alumina/diamond polishes.

This was done to get a well polished and a smooth surface required for the further characterization of the samples. Figure 5.7 shows the polished sample.

Similarly all the samples were polished for a considerable time, over and over again until a very fine and smooth surface was obtained for the further analysis.

5.7 Characterization

- Microstructural analysis
- Hardness Measurement
    1. Microhardness measurement
    2. Bulk Hardness measurement

5.7.1 Micro structural analysis

The well-polished samples were then observed under an optical microscope. Micrographs were taken with the help of CCD camera attached to the optical microscope and are further viewed on computer with optical image analyzer software at magnification of 200X and 400X for all the different samples.

5.7.2 Microhardness measurement

Well polished samples were then further used for the vicker microhardness testing. Hardness value was measured using formula

$$\mathbf{DPH} = \frac{\mathbf{1.854P}}{\mathbf{L^2}}$$

Where

P - applied load, kg

L - average length of diagonals, mm

Firstly sample was placed under the microscope (attached with instrument) for the proper selection of the area to take the hardness value. Indentation was made with the help of diamond indenter at load 0.100 Kg for 15 seconds. Diagonal length of the indentation was measured with the help of microscope (attached with instrument). 3 readings to each sample had been taken to get an average value of hardness. Figure 5.8 showing the microhardness tester used to get hardness values.

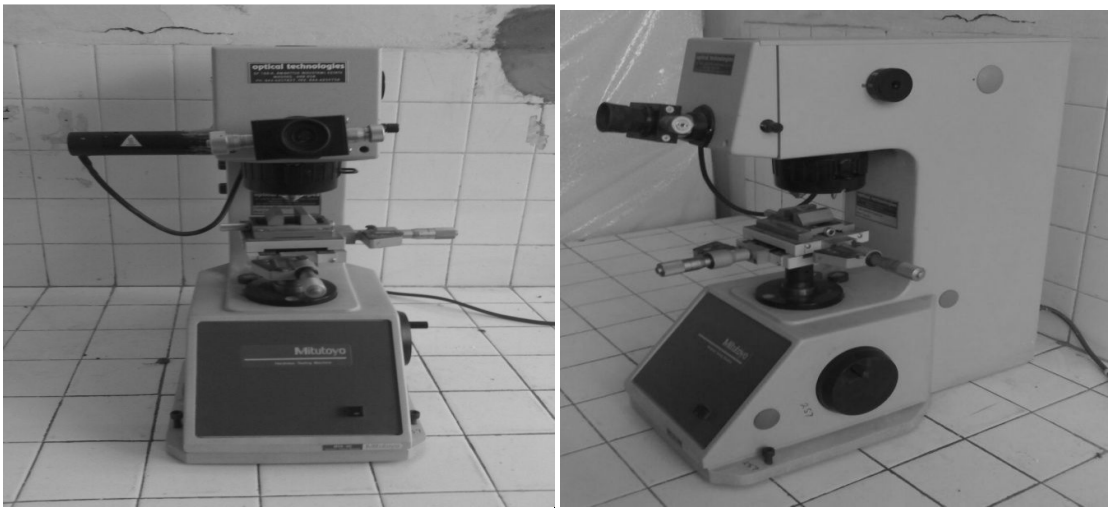

Figure 5.8 showing the front and side view of vicker microhardness tester (Mitutoyo company) used in the microhardness measurement

5.7.3 Bulk hardness measurement

Sample shown in figure 5.4 were used for Rockwell hardness testing. Machine was standardize with the help of standard steel sample. Firstly sample was properly grinded to get the smooth and parallel surface. Sample was then placed on table of Rockwell tester (FIE company). We had chosen steel ball indenter of size 1/16. A load of 10kg is firstly applied which causes an initial penetration. Then, the dial is set to zero and load of 100kg is applied. Upon removing the load the dial of the Rockwell tester gives the direct reading on Rockwell B scale. Similarly process is repeated 3 times each for each sample to get an average value of Rockwell hardness (RHB).

CHAPTER – 6

RESULT AND DISCUSSION

For the analyzing we had divided the whole 32 samples compositions into the 5 different sets. We analyzed the each set individually and also by comparison with each other. We had tried to relate microstructure analysis with the microhardness and bulk hardness.

6.1 Set 1

In set 1 Al-Si alloy with single alloying element had been studied

Table 6.1 showing the composition of elements in set 1

Elements	**Al (wt%)**	**Al-Si Master Alloy (wt%)**	**Bi (wt%)**	**Ca (wt%)**	**Sn (wt%)**	**Pb (wt%)**	**Cd (wt%)**
Sample-1	64	41.4	--	--	--	--	--
Sample-2	64	41.4	4.5	--	--	--	--
Sample-3	64	41.4	--	4.5	--	--	--
Sample-4	64	41.4	--	--	4.5	--	--
Sample-5	64	41.4	--	--	--	4.5	--
Sample-6	64	41.4	--	--	--	--	4.5

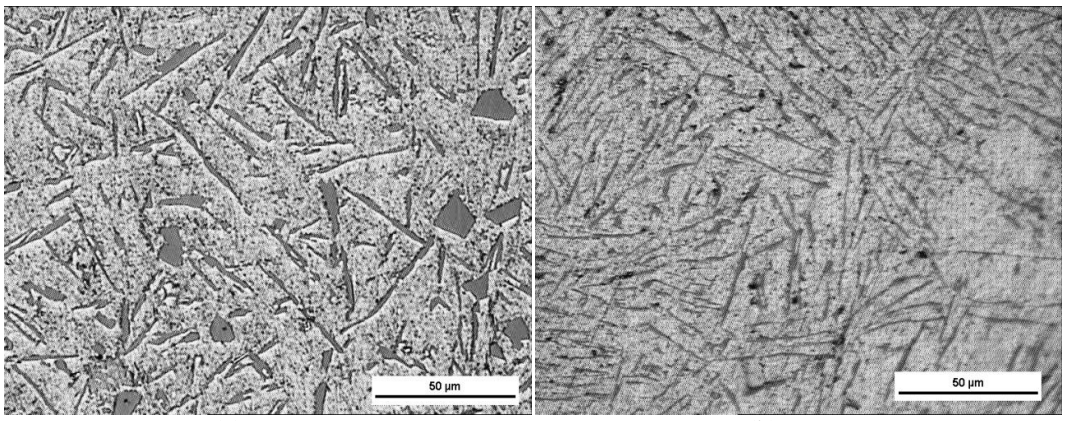

(a) (b)

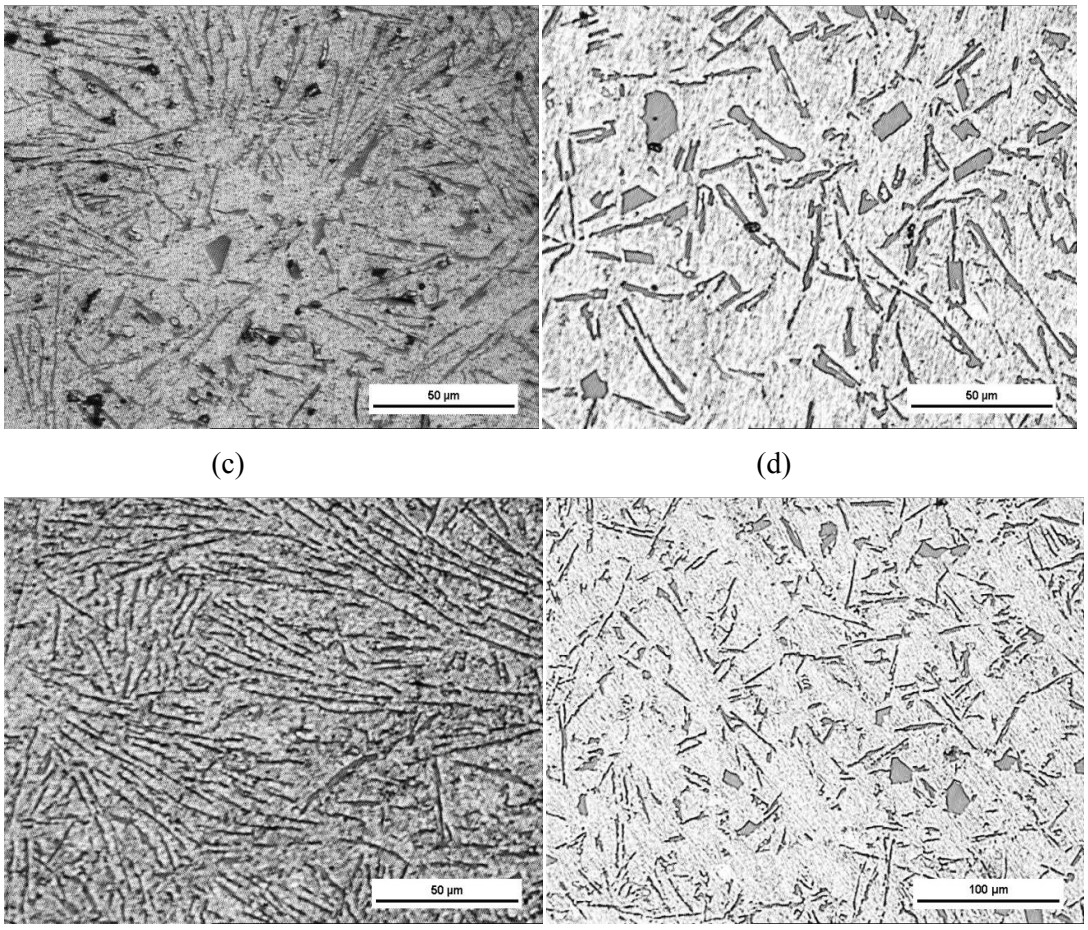

(c) (d)

(e) (f)

Figure 6.1(a-f) showing the microstructures of sample1, sample2, sample3, sample4, sample5 and sample6 respectively at magnification 200X.

6.1.1 Microstructural analysis

Microstructure 6.1(a) shows the eutectic composition of Al-Si alloy without any alloying element [11]. Distributions of the silicon needles are uniform over entire sample but the sizes of silicon needles are not refined. Also the primary silicon coarse particles are present throughout the sample. Figure 6.1(b) shows the alloying effect of Bi in the sample. In this microstructure the silicon needles are refined over the entire sample. However, the presence of large number of α-Al grains is also visible in the sample. In the microstructure 6.1(c) shows the effect of Ca on the cast sample [9]. The silicon needles and α-Al grains are visible over entire sample. Primary silicon particles are present randomly in the sample. Microstructure 6.1(d) shows the effect of 4.5 wt% Sn on the silicon needles which are distributed throughout the sample but the structure is not so refined primary silicon particles

are also seen [13]. On addition of Pb (fig. 6.1(e)) drastic change in the needle structure had been found. Si needles got more refined as well as long while distributed homogeneously in the entire sample. Figure 6.1(f) has fiber like silicon phase distributed all over the sample but the α-Al phase are present at some positions where the distribution is not so good.

Analyzing the micrographs it had been found that the morphology of silicon changes from needle like structure to the thick fibrous on addition of Sn (fig. 6.1(d)) and Cd (fig. 6.1(f)). However, it got more refined in the case of adding Bi (fig. 6.1(b)), Ca(fig. 6.1(c)) and Pb(fig. 6.1(e)).

6.1.2 Microhardness

Table 6.2 showing vicker microhardness number of the samples

Sample Name	VHN-1	VHN-2	VHN-3	Average
Sample-1	59.12	61.29	61.29	60.56
Sample-2	53.26	49.83	59.11	54.06
Sample-3	61.28	63.58	61.28	62.04
Sample-4	57.06	59.11	59.11	58.42
Sample-5	59.11	63.58	63.58	62.09
Sample-6	59.11	59.11	59.11	59.11

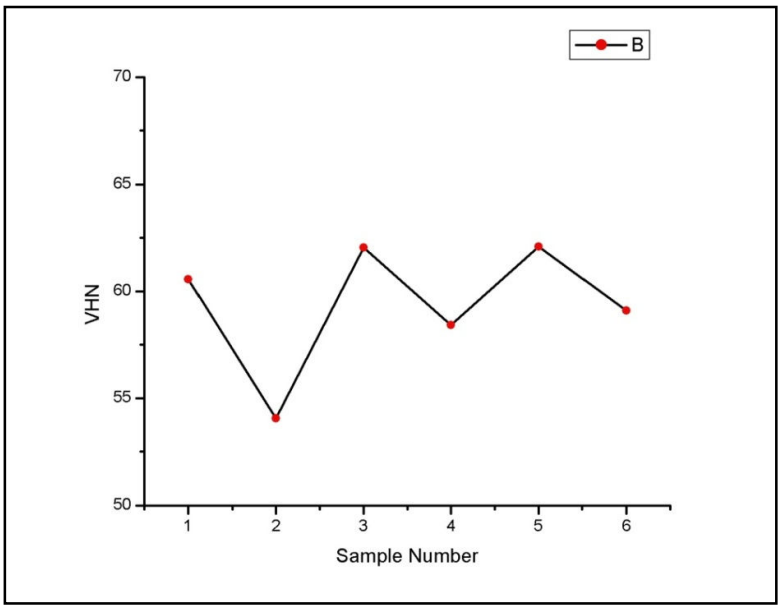

Figure 6.2 showing the graph of varying VHN with samples composition taken in table [6.1]

If we compare the microhardness results with the microstructures we can say that micro hardness value 54.06VHN of the sample-2 is less because the large numbers of α-Al grains are present through out the sample (fig 6.1(b)). The hardness of sample-4, sample-6 is comparable due to the lack of presence of refined silicon structure in the sample as shows in respective figures 6.1(d), and 6.1(f). Hardness of sample-1 and sample-3 is also good due to fine structure of silicon needles but not as fine as in sample-5. Figure 6.2 showing the graph between samples composition and hardness value (VHN). In this set sample number 5 shows maximum microhardness value 62.09VHN because the structure of silicon needles are much refined and homogenously distributed throughout the sample.

6.1.3 Bulk hardness

Table 6.3 showing the HRB number of the samples

Sample Name	HRB-1	HRB-2	HRB-3	Average
Sample-1	90	92	86	89.33
Sample-2	72	75	80	75.67
Sample-3	80	84	83	82.33
Sample-4	70	68	71	69.66
Sample-5	86	87	88	87.00
Sample-6	85	82	87	84.67

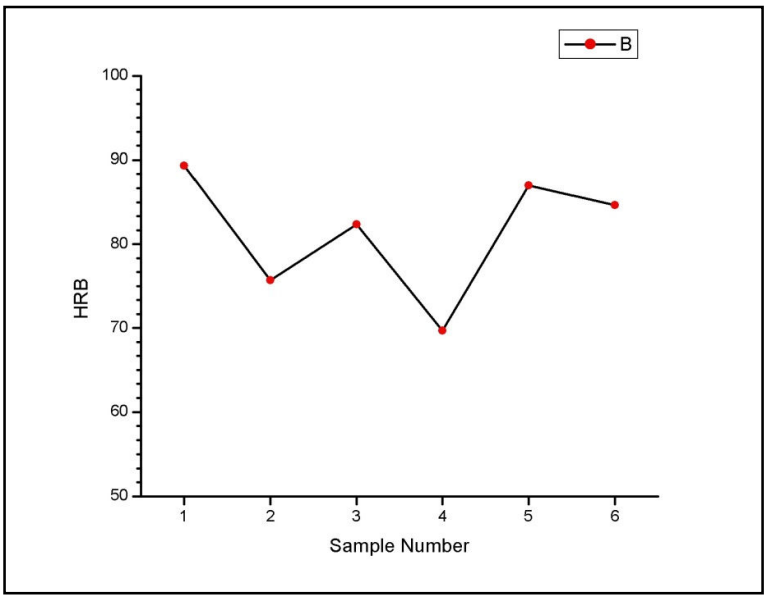

Figure 6.3 showing the varying HRB with samples composition taken in table [6.1]

Sample number 5 and 1 have good hardness values 87.00HRB and 89.33HRB microstructure of both these samples have fine and well distributed silicon needles. But the presence of primary silicon is observed in sample 1. Sample number 3 and 6 also shows good hardness values but the presence of α-Al grains making these samples soft as compare to previous one. Sample number 4 have the least hardness value 69.66HRB in this set. If we compare the microstructure of the sample with other samples we can see clearly that the α-Al grains are distributed randomly over the entire sample. However, the nature of curve is similar for both bulkhardness and microhardness.

6.2 SET 2

In set 2 Al-Si eutectic alloy with two alloying element had been studied.

Table 6.4 showing the chemical composition of the samples

Elements	**Al (wt%)**	**Al-Si Master Alloy (wt%)**	**Bi (wt%)**	**Ca (wt%)**	**Sn (wt%)**	**Pb (wt%)**	**Cd (wt%)**
Sample-7	64	41.4	4.5	4.5	--	--	--
Sample-8	64	41.4	4.5	--	4.5	--	--
Sample-9	64	41.4	4.5	--	--	4.5	--
Sample-10	64	41.4	4.5	--	--	--	4.5
Sample-11	64	41.4	--	4.5	4.5	--	--
Sample-12	64	41.4	--	4.5	--	4.5	--
Sample-13	64	41.4	--	4.5	--	--	4.5
Sample-14	64	41.4	--	--	4.5	4.5	--
Sample-15	64	41.4	--	--	4.5	--	4.5
Sample-16	64	41.4	--	--	--	4.5	4.5

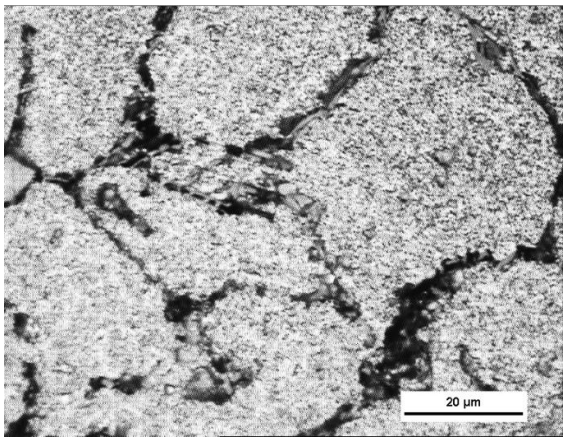

(a)

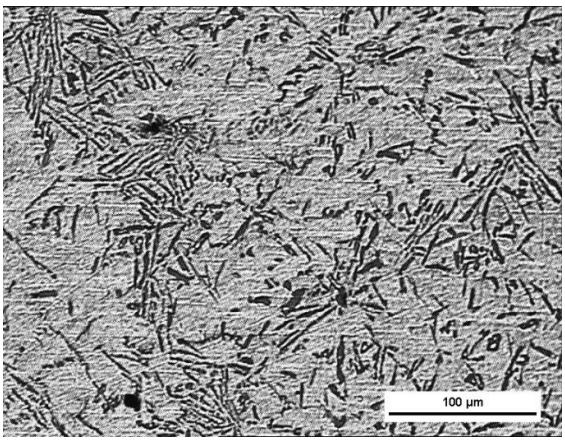

(b)

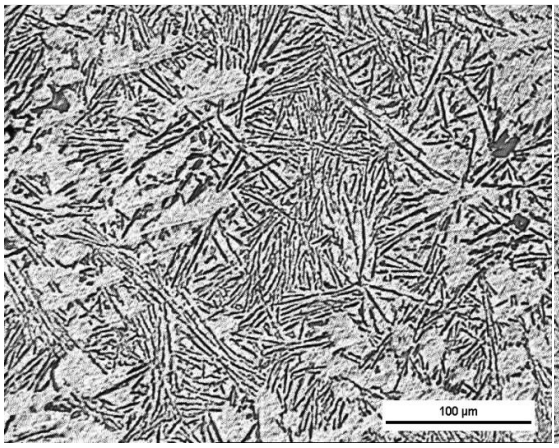

(c)

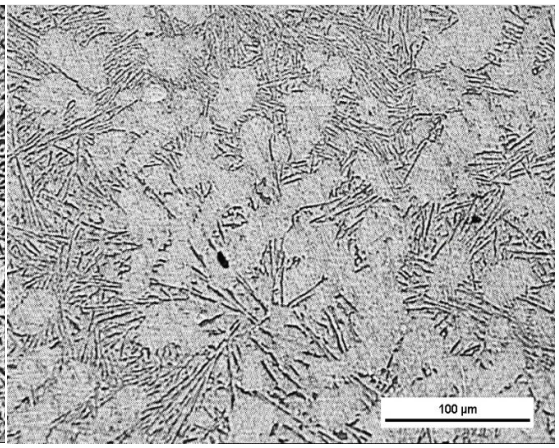

(d)

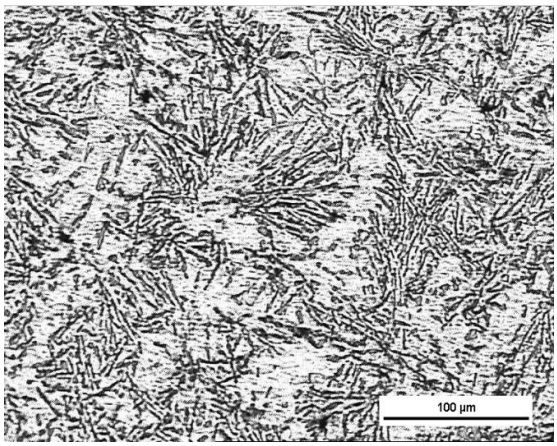

(e)

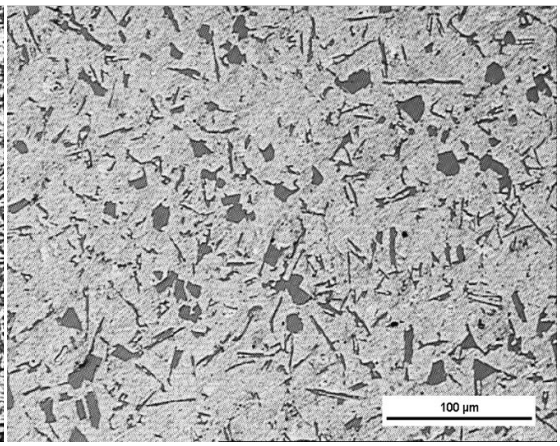

(f)

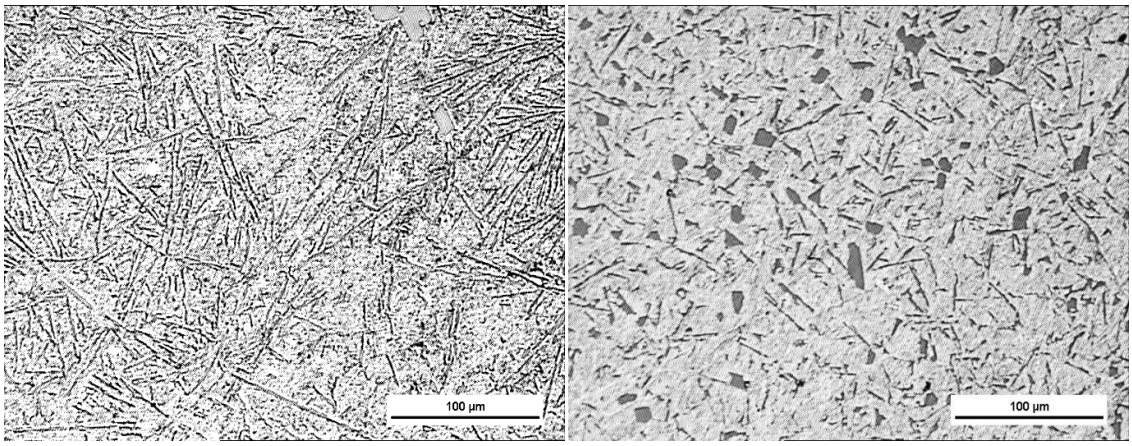

(g) (h)

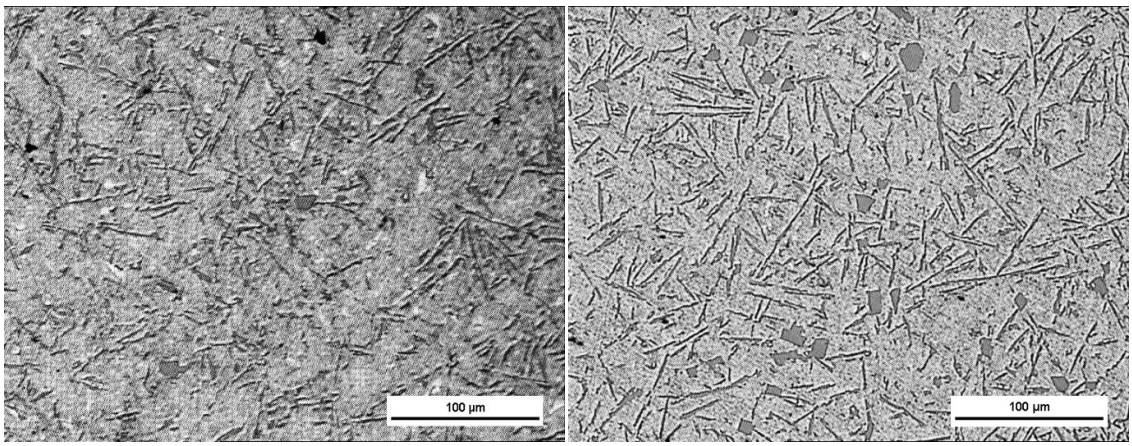

(i) (j)

Figure 6.4(a-j) represent the microstructures of samples from sample (7-16) respectively

6.2.1 Microstructure analysis

From figure 6.4(a) shows the effect of Bi and Ca, we can interpret that very small amount of silicon is distributed along the grain boundaries of the alpha-aluminum. Grain boundaries of aluminum are visible after etching the sample with Keller's reagent (20 ml distilled H_2O + 20 ml HNO_3 + 20 ml HCl + 5 ml HF). In microstructure 6.4(b) shows the effect of Bi and Sn, silicon needles are distributed randomly as well as α-Al phase [6]. From the microstructural analysis 6.4(d) of sample-10 it has been observed that fine silicon needles are randomly distributed over entire sample in between the area where α-Al grains are present due to the alloying effect of Bi and Cd [6]. The microstructure 6.4(e) showed the effect of Ca and Sn and it is observed that bunches of silicon is embedded around the α-Al phase. There are some

areas in the samples where the distribution is good but the α-Al phase present in this microstructure is less than 6.4(d). Microstructure 6.4(f) shows the effect of Ca and Pb, presence of primary silicon particles are all over the microstructure[13]. In microstructure 6.4(g) effect of Ca and Cd shows the fine refinement of silicon needles as well as well the better distribution over the entire sample. From the microstructure 6.4(h) the well distributed primary Si is present in the entire sample and found that on addition of Sn and Pb the spacing between the needles also increases. In microstructure 6.4(i) the distribution of silicon is not uniform due to effect of Sn an Cd alloying elements. Structure of the silicon is refined but the distribution is not so good. The presence of large number of α-Al phase is observed in the microstructure. Due to the effect of Pb and Cd in microstructure 6.4(j) needles of the silicon is long in size as compare to previous sample [13]. The presence of primary silicon is also there but randomly distributed.

While comparing the micrographs of set 2 distribution and refinement of silicon needles in microstructure 6.4(g) is maximum, the least distribution of silicon needles and presence of maximum α-Al grains in the microstructure 6.4(a). The distribution of silicon needles in microstructures 6.4(b), 6.4(c), 6.4(d) and 6.4(f) is also good and the presence of α-Al phase in little amount is also there over entire sample. The uniform distributions of primary silicon particles are present in microstructures 6.4(f), 6.4(h) and 6.4(j). Micrograph 6.4(i) shows the presence of α-Al grains over entire sample.

6.2.2 Microhardness analysis

Table 6.5 showing vicker microhardness number of the samples

Sample Name	VHN-1	VHN-2	VHN-3	Average
Sample 7	42.56	45.26	42.56	43.46
Sample 8	55.11	59.11	59.11	57.77
Sample 9	59.11	61.28	61.28	60.55
Sample 10	59.11	59.11	55.11	57.77
Sample 11	57.06	59.11	59.11	58.42
Sample 12	63.58	57.06	57.06	59.23
Sample 13	63.58	66.00	63.58	64.38
Sample 14	57.06	61.29	55.11	57.82

Sample 15	53.26	53.26	51.50	52.67
Sample 16	57.06	55.11`	55.11	55.76

In microhardness analysis we can see clearly from figure 6.5 that sample number 13 have better hardness value 64.38VHN with comparison to other samples. The reason being, the well refined and well distributed silicon needles in the microstructure 6.4(g). The presence of α-Al phase in comparison to sample number 7, 8, 14 and 15 is very less as seen in figures 6.4(a), 6.4(b), 6.4(h) and 6.4(i) respectively. Sample number 7 have very less microhardness value 46.64VHN in comparison to other sample because the silicon is present in the grain boundaries of aluminum and also the α-Al phase present over all the sample as seen in figure 6.4(a). Due the presence of both fine silicon needles and α-Al phase in the

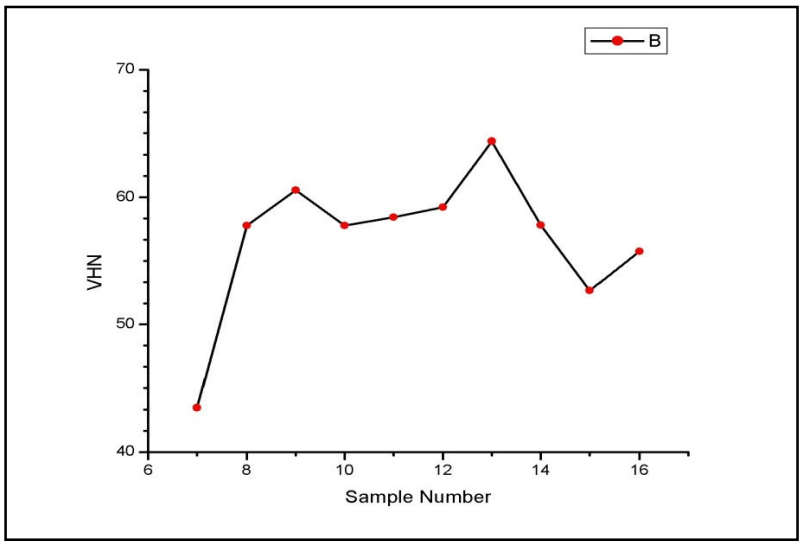

Figure 6.5 showing the graph of variation in VHN with samples composition taken in table [6.4]

sample number 11 and 12 hardness values 58.42VHN and 59.23VHN are comparable with relation to there microstructure 6.4(e) and 6.4(f) respectively. Sample number 9 also gives good hardness values 60.55VHN because of good distribution of silicon in microstructure as well as very less amount of α-Al phase is present as shown in figure 6.4(f).

6.2.3 Bulk hardness

Table 6.6 showing Rockwell hardness number of the samples

Sample Name	HRB-1	HRB-2	HRB-3	Average
Sample 7	31	30	30	30.33
Sample 8	30	38	42	36.66
Sample 9	66	66	70	67.33
Sample 10	63	45	52	53.33
Sample 11	73	77	74	74.67
Sample 12	83	87	85	85.00
Sample 13	89	88	89	88.66
Sample 14	78	78	79	78.33
Sample 15	49	54	56	53.00
Sample 16	92	89	88	89.66

It is clear from graph 6.6 that bulk hardness of samples number 13 and 16 have maximum hardness value 88.66HRB and 89.66HRB by relating these hardness values with microhardness graph shown in figure 6.5 and microstructures 6.4(g) and 6.4(j) we can say that distribution of silicon needles in both samples are homogenous. However in sample 13 the presence of α-Al grains is more than sample 16 but it is comparatively very less than other samples in this set.

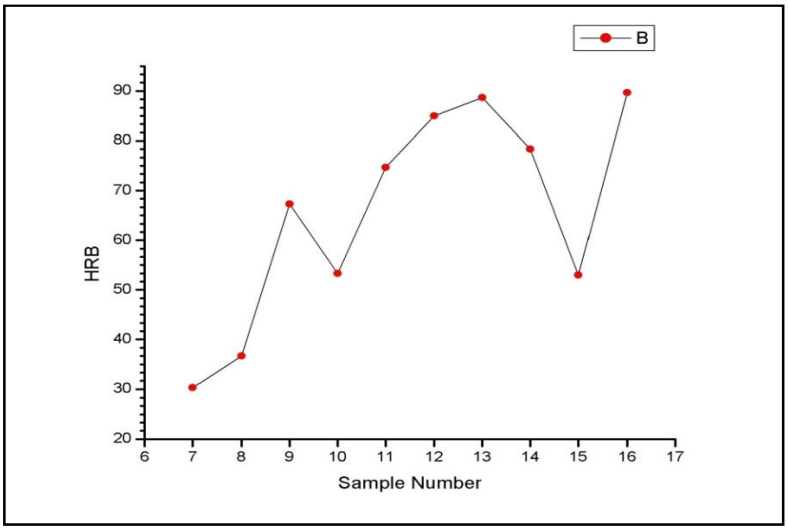

Figure 6.6 showing the varying HRB with samples composition taken in table [6.4]

Sample number 12 also have good hardness values 85HRB but presence of primary silicon particles and α-Al phase is more in this case than sample number 13 and 16. If we compare the microstructure 6.4(e) and 6.4(h) of the sample number 11 and 14 we can clearly see the bunches of silicon needles structure in sample 11 as that of sample number 14 but the distribution of homogenous soft α-Al grains in sample 14 reduces the bulk hardness values of sample 14 compare to sample 11. Samples number 7 and 8 have least values of hardness 30.33HRB and 36.66HRB respectively in these set. In the microstructure 6.4(a) and 6.4(b) there is a homogenous distribution of α-Al grains throughout the sample which makes these sample soft compare to others.

6.3 SET 3

In set 3 Al-Si eutectic alloy with three alloying element had been studied.

Table 6.7 showing the chemical composition of the samples

Elements	Al (wt%)	Al-Si Master Alloy (wt%)	Bi (wt%)	Ca (wt%)	Sn (wt%)	Pb (wt%)	Cd (wt%)
Sample 17	64	41.4	4.5	4.5	4.5	--	--
Sample 18	64	41.4	4.5	4.5	--	4.5	--
Sample 19	64	41.4	4.5	4.5	--	--	4.5
Sample 20	64	41.4	4.5	--	4.5	4.5	--
Sample 21	64	41.4	4.5	--	4.5	--	4.5
Sample 22	64	41.4	4.5	--	--	4.5	4.5
Sample 23	64	41.4	--	4.5	4.5	4.5	--
Sample 24	64	41.4	--	4.5	4.5	--	4.5
Sample 25	64	41.4	--	4.5	--	4.5	4.5
Sample 26	64	41.4	--	--	4.5	4.5	4.5

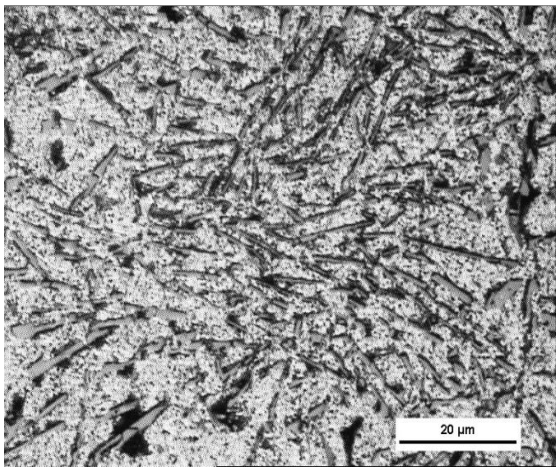

(a)

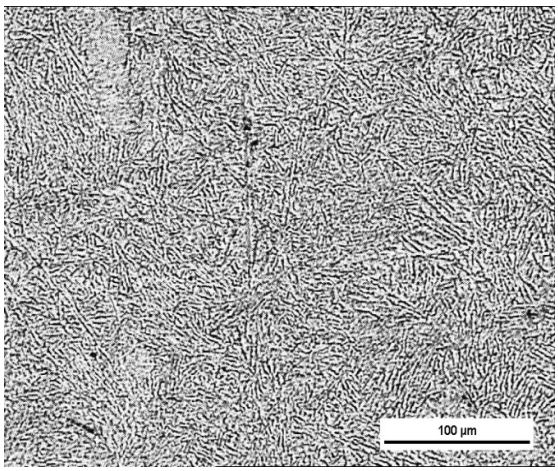

(b)

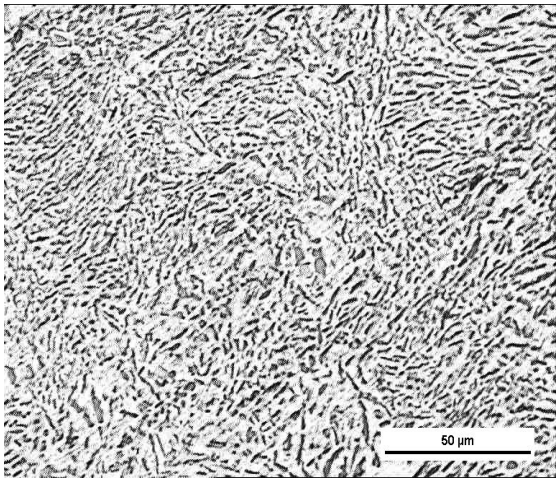

(c)

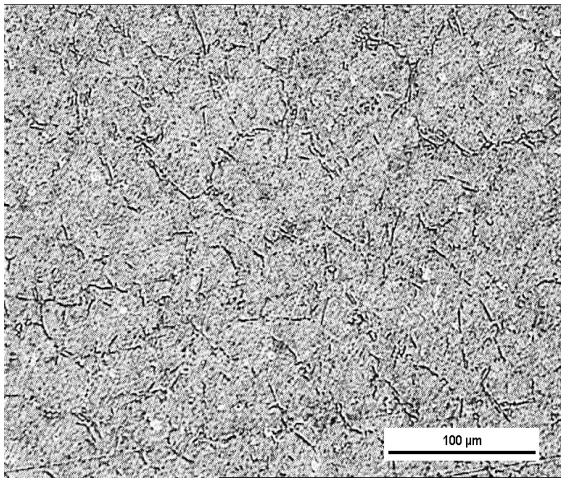

(d)

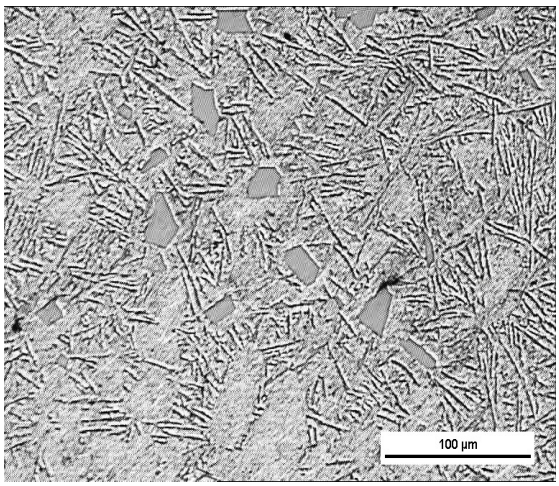

(e)

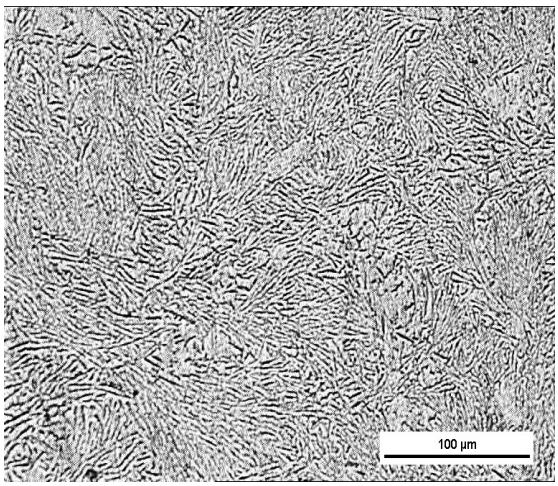

(f)

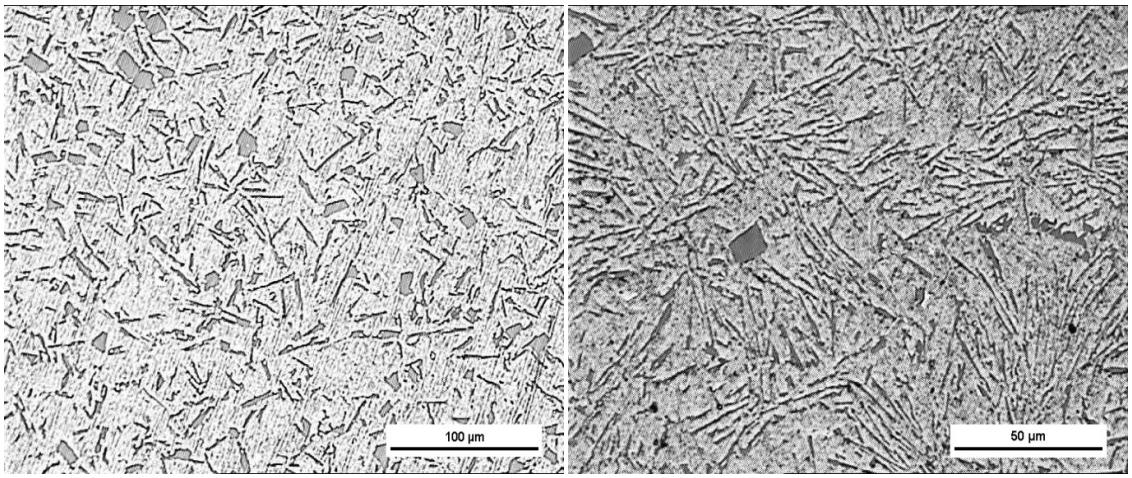

(g) (h)

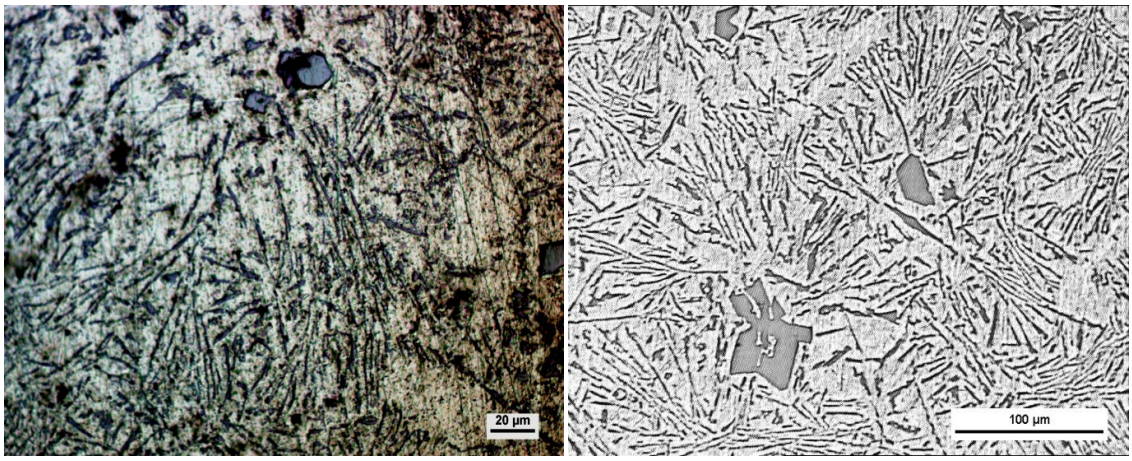

(i) (j)

Figure 6.7(a-j) represent the microstructures of samples from sample (17-26) respectively

6.3.1 Microstructure analysis

In the microstructure 6.7(a) effect of Bi, Ca and Sn shows that the silicon is distributed homogenously over some places over the samples but α-Al phase is also present in the microstructure. This aluminum phase is present in the whole sample like island. The sizes of silicon needles are refined in the structure. In the microstructure 6.7(b) due to effect of alloying elements Bi, Ca and Pb the distribution of silicon needles over whole sample has been observed [16]. The needles of the silicon are also refined and well distributed. The micrograph 6.7(c) of this sample shows the effect of alloying elements Bi, Ca and Cd due to the fact that distribution of silicon morphology is very homogenous and continuous in the

alloy [16]. The microstructure 6.7(d) shows that the segregation of Si and alloying element along the grain boundaries on addition of Bi, Sn and Pb. Aluminum grains are clearly visible in the sample. In the microstructure 6.7(e) there is the presence of primary silicon particles distributed over whole sample however the distribution is not so uniform. In this micrograph silicon needles are present with α-Al phase on addition of Bi, Sn and Cd. However on the addition of Pb instead of Sn in the Al-Si-Pb-Bi-Cd (figure 6.7(f)) structure of silicon needles obtained are well refined [16]. The silicon needles have been refined to some extent but the presence of large amount of primary silicon particles can also be seen in the micrograph 6.7(g) due to the effect of alloying elements Ca, Sn and Pb. In microstructure 6.7(h) the distribution of silicon needles are very good due to effect of Ca, Sn and Cd. While comparing it with previous microstructure, the silicon needle are much fine. Also the presence of primary silicon particles over the whole sample can be observed easily. In Ca, Pb and Cd sample number 25 eutectic silicon needles present in between the α-Al grains in the micrograph 6.7(i). Coarse silicon particles along with the silicon needles have been observed in the microstructure 6.7(j) of sample Sn. Pb and Cd.

Microstructure 6.7(e) and 6.7(i) shows the good refinement and uniform distribution of silicon needles over entire sample however the distribution of silicon needles in 6.7(f) is also very good. In micrograph 6.7(d) there is least distribution of silicon needles over entire sample also the segregation of silicon along the grain boundaries is also observed in this microstructure. The presence of α-Al grains are observed in microstructures 6.7(d), 6.7(f), 6.7(g) and 6.7(j). The presence of primary silicon particles are also observed in microstructure 6.7(d).

6.3.2 Microhardness

Table 6.8 showing vicker microhardness number of the samples listed below

Sample Name	VHN-1	VHN-2	VHN-3	Average
Sample 17	57.06	55.11	59.11	57.09
Sample 18	61.28	59.11	63.58	61.32
Sample 19	66.00	68.56	63.58	66.04
Sample 20	46.71	45.26	48.23	46.73

Sample 21	57.06	57.06	55.11	56.41
Sample 22	57.06	59.11	61.28	59.51
Sample 23	55.11	55.11	55.11	55.11
Sample 24	55.11	53.26	61.28	56.55
Sample 25	74.15	71.28	68.56	71.33
Sample 26	57.06	57.06	59.11	57.74

It is clear from the figure 6.8 that sample number 25 have maximum value of microhardness 71.33VHN with relation to its microstructure 6.7(i) we can see easily the distribution of silicon needles in this sample is quite good over some areas in the microstructure also the structure of silicon needles are also very refined. Sample number 19 also shows good microhardness value 66.04VHN with respect to its microstructure 6.7(c). In the microstructure the distribution of silicon are very uniform also the silicon needles are very refine. Sample number 18 and sample number 22 shows good microhardness values 61.32VHN and 59.11VHN. The microstructure 6.7(b) of sample 18 has very refined silicon needles with α-Al grains present randomly in very less amount.

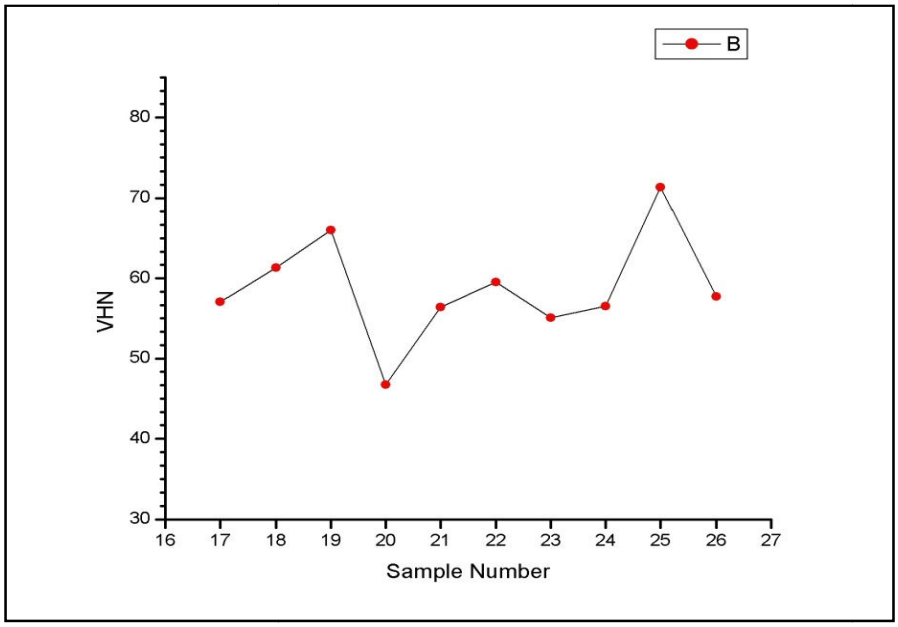

Figure 6.8 showing the graph of varying VHN with samples composition taken in table [6.7]

Sample number 22 have homogenous structure of silicon needles present over entire sample with presence of α-Al grains in micrographs homogenously. Sample number 17, 21, 23 and 26 (according to micrographs 6.7(a), 6.7(e), 6.7(g) and 6.7(j) respectively) shows the average values of microhardness having α-Al phase distributed randomly in these samples. Also the presence of primary silicon particles is observed in sample number 21, 23 and 26 also the silicon is not so refined but distributed homogenously among most of samples. Figure 6.8 shows that sample number 20 have minimum value of microhardness 46.73VHN (figure 6.7(d)) we see easily that only α-Al grains are present through out the sample and small amount of silicon segregate along the grain boundaries of aluminum.

6.3.3 Bulk hardness

Table 6.9 showing Rockwell hardness number of the samples

Sample Name	HRB-1	HRB-2	HRB-3	Average
Sample 17	83	80	85	82.66
Sample 18	89	90	92	90.33
Sample 19	90	90	91	90.33
Sample 20	35	37	34	35.33
Sample 21	76	77	76	76.33
Sample 22	93	91	92	92.00
Sample 23	80	82	84	82.00
Sample 24	76	74	77	75.67
Sample 25	90	91	90	90.33
Sample 26	86	83	89	86.00

In figure 6.9 the hardness values 90.33HRB, 90.33HRB, 92.00HRB and 90.33HRB of samples number 18, 19, 22 and 25 are very good. If we compare the microstructures 6.7(b), 6.7(c), 6.7(f) and 6.7(i) of these samples with the hardness values, we see the distribution and refinement of the silicon needles in all the samples are very good. The microhardness values of these samples are also very good and can be seen in figure 6.8. The bulk hardness values of samples number 17, 23 and 26 are also 82.66HRB, 82HRB and 86HRB also good by relating these hardness values with the microstructures 6.7(a), 6.7(g) and 6.7(j) of these

samples. The distribution of silicon needles are more distributed in sample in sample 26 but the presence of coarse silicon particles are also seen in this sample.

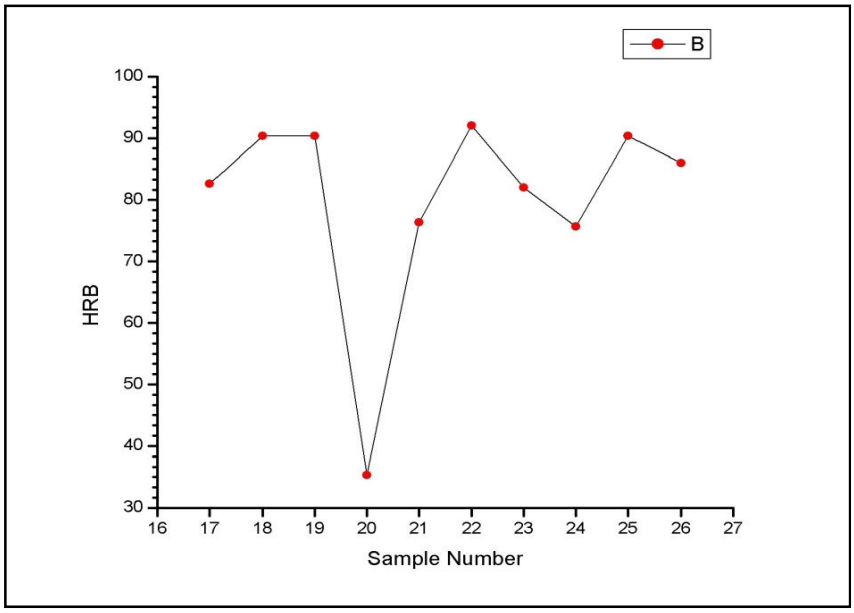

Figure 6.9 showing the varying HRB with samples composition taken in table [6.7]

Samples number 21 and 24 (micrograph 6.7(e) and 6.7(h)) have hardness value 76.33HRB and 75.67HRB respectively as the amount of α-Al grains are more in these samples as compare to other samples. Sample number 20 have least value of hardness 35.33HRB in this set (micrograph 6.7(d)). We can see clearly the uniform distribution of α-Al grains over the entire sample also silicon is segregated along the grain boundaries.

6.4 SET 4

In set 4 Al-Si eutectic alloy with four and five alloying element had been studied.

Table 6.10 showing the chemical composition of the samples

Elements	**Al (wt%)**	**Al-Si Master Alloy (wt%)**	**Bi (wt%)**	**Ca (wt%)**	**Sn (wt%)**	**Pb (wt%)**	**Cd (wt%)**
Sample-27	64	41.4	4.5	4.5	4.5	4.5	--
Sample-28	64	41.4	--	4.5	4.5	4.5	4.5

Sample-29	64	41.4	4.5	--	4.5	4.5	4.5
Sample-30	64	41.4	4.5	4.5	--	4.5	4.5
Sample-31	64	41.4	4.5	4.5	4.5	--	4.5
Sample-32	64	41.4	4.5	4.5	4.5	4.5	4.5

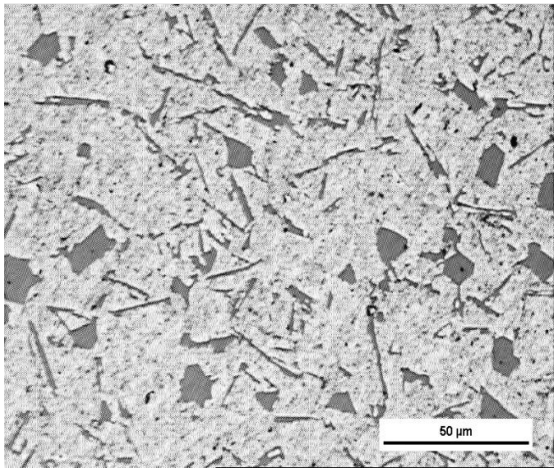

(a)

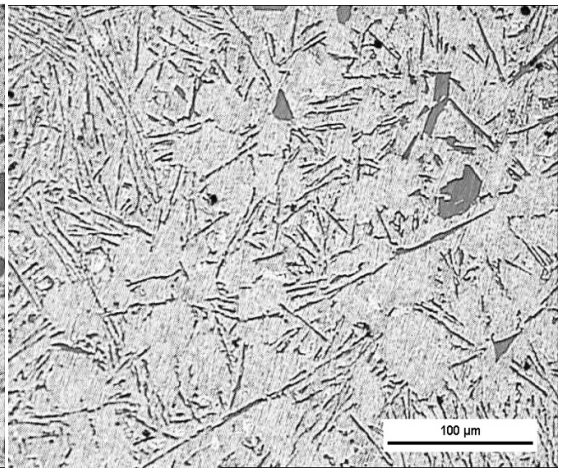

(b)

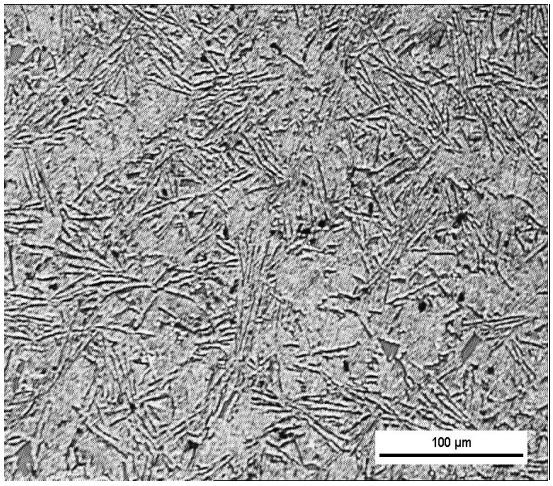

(c)

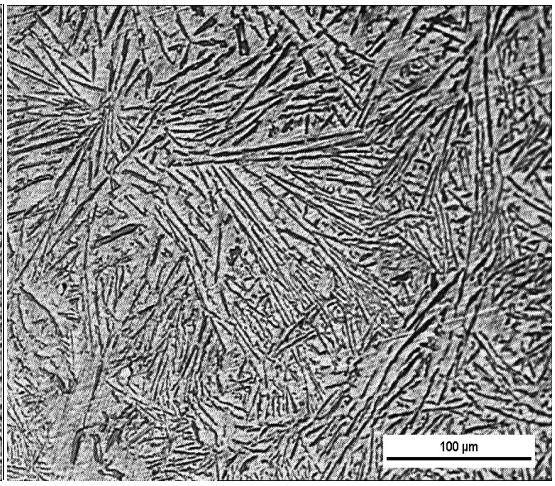

(d)

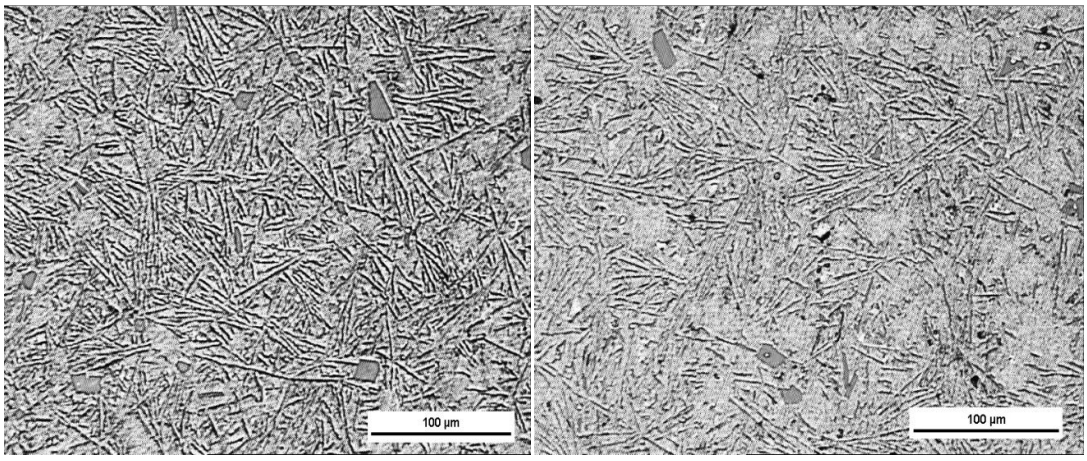

(e) (f)

Figure 6.10(a-f) represent the microstructures of samples from sample (27-32) respectively

6.4.1 Microstructure analysis

In the micrograph 6.10(a) the distribution of the silicon needles in the sample is not very good however; the distribution of the primary silicon is uniform over the entire sample as the effect of alloying elements Bi, Ca, Sn and Pb [11]. In the micrograph 6.10(b) alloying with elements Ca, Sn, Pb and Cd silicon needles obtained are sharp edged and distributed randomly. α-Al grains are surrounded by the sharp edge silicon needles. In the micrograph 6.10(c) refinement of silicon needles are not so good but the distribution of the silicon needles at some places in the sample is quite good this effect is due to presence of alloying elements Sn, Pb, Cd and Bi. The α-Al grains are present throughout the sample. In micrograph 6.10(d) the distribution of long and thin Si needles can be seen over the entire sample with no α-Al grain present. The distribution of the silicon needles over the most of the places in the sample is quite good as seen in micrograph 6.10(e) due to presence of alloying elements Cd, Bi, Ca and Sn. Primary silicon particles are also present in the sample but not homogenously. In micrograph 6.10(f) the needles morphology is similar to micrograph 6.10(e) however, the amount of α-Al grains has been increased throughout the sample. Micrograph 6.10(d) and 6.10(e) shows the refinement of silicon needles and distribution of silicon needles over the entire sample however, presence of α-Al grains is observed more in 6.10(e).

6.4.2 Microhardness analysis

Table 6.11 showing vicker microhardness number of the samples listed below

Sample Name	VHN-1	VHN-2	VHN-3	Average
Sample-27	57.06	61.29	55.11	57.82
Sample-28	61.28	61.28	61.28	61.28
Sample-29	57.06	57.06	57.06	57.06
Sample-30	68.56	61.28	59.11	62.98
Sample-31	74.15	71.28	68.56	71.33
Sample-32	61.28	57.06	59.11	59.15

From figure 6.11 we can predict easily that the sample number 31 have maximum microhardness value 71.33VHN among this set. In comparison to its microstructure 6.10(e) the distribution of silicon is homogenous at the most of the places of the sample however the α-Al phases are also present in the sample randomly.

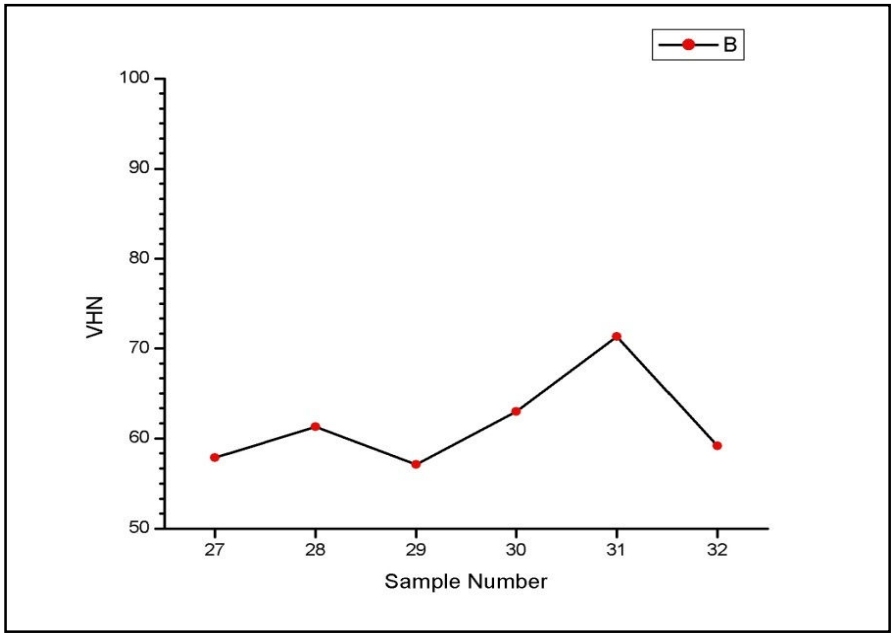

Figure 6.11 showing the graph of varying VHN with samples composition taken in table [6.10]

Sample number 28 and 30 also shows the good microhardness value 61.28VHN and 62.98VHN. The microstructures of these samples 6.10(b) and 6.10(d) respectively have well distributed silicon needles throughout the sample while α-Al grains are also present randomly over the samples. Sample number 27, 29 and 32 shows the average values of microhardness

57.82VHN, 57.06VHN and 59.15VHN respectively silicon needles are not so refined but distributed uniformly over some areas of the samples while α-Al grains present throughout the sample.

6.4.3 Bulk hardness

Table 6.12 showing Rockwell hardness number of the samples

Sample Name	HRB-1	HRB-2	HRB-3	Average
Sample-27	81	81	78	80.00
Sample-28	81	78	80	79.66
Sample-29	79	81	78	79.33
Sample-30	89	86	89	88.00
Sample-31	80	84	83	82.33
Sample-32	70	75	72	72.33

It is clear from graph 6.11 that the hardness value 88HRB of sample number 30 is maximum in this set. By relating it with the microstructure 6.11(e) it can be seen clearly that the silicon needles are distribution over the entire sample. Hardness values 80HRB and 82.33HRB of sample 27 and 31 are also comparable.

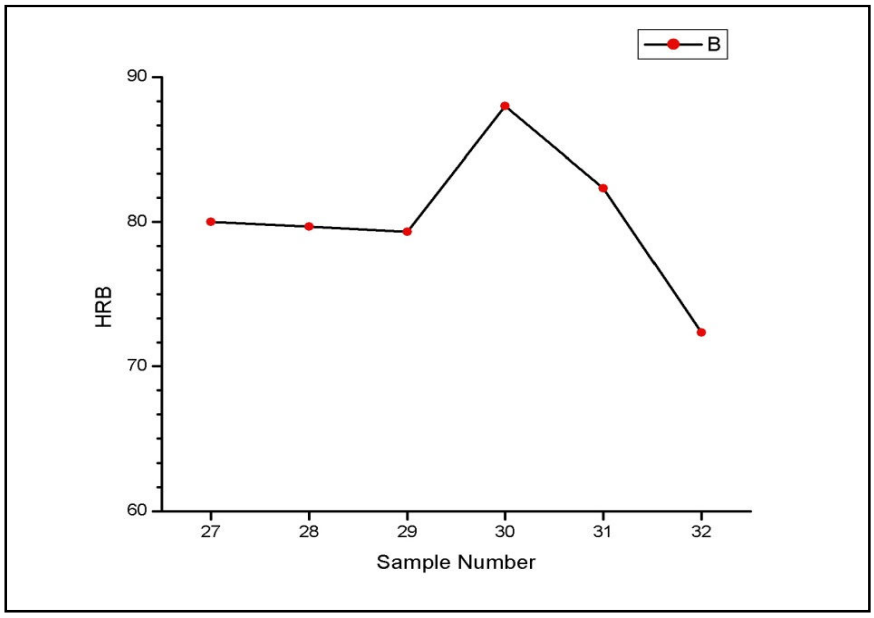

Figure 6.12 showing the varying HRB with samples composition taken in table [6.10]

Micrographs 6.10(a) and 6.10(e) both have well distributed silicon needles over the whole sample number 31 have more refine silicon needles structure than 27. However the presence of α-Al phase in sample 27 is more compare to sample 31. Sample number 28 and 29 have comparable hardness values 79.66HRB and 79.33HRB. In both microstructures the presence of α-Al grains are more than previous samples but the refinement of silicon needles are more in sample number 29. Sample number 32 have least value of hardness 72.33HRB. While relating it with the microstructure 6.10(f) it is clearly seen that the α-Al grains are more in this micrograph as compare to others.

CONCLUSIONS

Al-Si eutectic alloys have been prepared by casting technique using the combination of five different alloying elements Bi, Cd, Ca, Sn and Pb. The affect of different combinations of alloying elements have been studied with the help of micrographs. Moreover, for analytical data the microhardness and bulk hardness of each sample have been taken randomly. After analyzing the results following conclusions can be drawn.

1. On simple addition of single alloying elements in Al-Si base alloy, Pb gives the best results among all the other used alloying elements for grain refinement.

2. Using Al-Si-Bi base alloy an addition of Ca and Sn tend to decrease mechanical properties of the alloy. On the microstructural analysis it had been found that Si segregate along the Al grain boundaries (Figure 6.4(a)) on addition of Ca in this alloy, while Sn increases amount of α-Al grains in the sample(Figure 6.4(b)).

3. In Al-Si-Ca base alloy, an addition of Cd gives the best results in microstructural analysis as well as in both the hardness testings than other alloying elements.

4. Drastic increase in the hardness values has been found when fourth alloying element Ca or Cd added to base alloy Al-Si-Pb-Bi. This is due to the fact that Ca and Cd reduces the segregation of Si around the Al grains.

5. On addition any one (Pb,Sn,Cd) of third alloying element to base alloy Al-Si-Bi-Ca the we observed thet silicon needles got refined and the interspacing between the Si needles also decreases which leads to good hardness results.

REFERENCES

1. Li Xin-tao *, Li Ting-ju, Li Xi-meng, Jin Jun-ze Study of ultrasonic melt treatment on the quality of horizontal continuously cast Al–1%Si alloy Received 14 May 2005; accepted 26 August 2005 Ultrasonic's Sonochemistry 13 (2006) 121–125.

2. Z.Y. Ma, S.R. Sharma, and R.S. Mishra Microstructural Modification of As-Cast Al-Si-Mg Alloy by Friction Stir Processing available online on sciencedirect.com. VOLUME 37A, NOVEMBER 2006—3323

3. Peter Szarvasy, Jozef Petrík, Jozef Cubek Al-Si COPPER ALLOYS FOR BEARINGS *accepted for publication: 2000-05-16* MATERIAL IN TEHNOLOGIJE 35 (2001) 1-2

4. Xiufang Bian, Weimin Wang Thermal-rate treatment and structure transformation of Al–13 wt.% Si alloy melt Received 24 September 1999; received in revised form 15 December 1999; accepted 19 January 2000 Materials Letters 44_2000.54–58

5. S.A. Kori, T.M. Chandrashekharaiah Studies on the dry sliding wear behaviour of hypoeutectic and eutectic Al–Si alloys. Wear 263 (2007) 745–755

6. LI Wei, FAN Hongyuan, ZHANG Xianju, and SHEN Baoluo Effect of barium on the refinement of primary aluminum and eutectics in a hypoeutectic Al-Si alloy RARE METALS Vol. 22, No. 3, Sep 2003, p. 192.

7. A.K. Prasada Rao, Karabi Das, B.S. Murty, M. Chakraborty Effect of grain refinement on wear properties of Al and Al–7Si alloy Wear 257 (2004) 148–153

8. A. Knuutinen, K. Nogita, S.D. McDonald and A.K. Dahle, *Modification of Al–Si alloys with Ba, Ca, Y and Yb*, Journal of Light Metals 1 (2001) 229–240.

9. N. Saheb, T. Laoui, R. Daud, R .Y Ahaya, and S. Radiman Microstructure and hardness behaviours of Ti-containing Al-Si alloys PHILOSOPHIMCAALG AZINAE, 2002, VOL. 82, No. 4, 803-814

10. Dheerendra Kumar Dwivedi, A. Sharma and T. V. Rajan INFLUENCE OF SILICON MORPHOLOGY AND MECHANICAL PROPERTIES OF PISTON ALLOYS Materials and Manufacturing Processes, 20: 777–791, 2005

11. K T Kashyap and T Chandrashekar Effects and mechanisms of grain refinement in aluminium alloys Bull. Mater. Sci., Vol. 24, No. 4, August 2001, pp. 345–353.

12. Shufang Yao1,2), Weimin Mao1), Xueyou Zhong1), Kaike Cai1), Zidong Wang1), Lei Mao2), and Juxiang Yang3) Application of CX-type modifiers in Al-Si alloys Journal of University of Science and Technology Beijing Volume 10, Number 2, April 2003, Page 34

13. H. Liao and G. Sun Influence of boron on the microstructure and mechanical properties of Al –11.6Si – 0.4Mg casting alloy modified with strontium Materials Science and Technology April 2004 Vol. 20 521

14. M. A. Moustafa, F. H. Samuel and H. W. Doty Effect of solution heat treatment and additives on the hardness, tensile properties and fracture behavior of Al-Si (A413.1) automotive alloys Journal Of Materials Science 38 (2003) 4523 – 4534

15. H.S. Kang, W.Y. Yoon, K.H. Kim, M.H. Kim, Y.P. Yoon, I.S. Cho Effective parameter for the selection of modifying agent for Al–Si alloy Materials Science and Engineering A 449–451 (2007) 334–337

16. S.N. Ojha, G. Diner, Y.Lu, J. Reye and S.N Tewari macrosegration caused by thermosolutal convection during directional solidification of Pb-Sb alloys. Metallurgical and Materails Transaction A, Volume 30A, August 1999, Page 2167

17. A. Upadhayaya, N.S Mishra, S.N. Ojha Microstructural control by spray forming and wear characterstic of babbit alloy, Journal of Material science, Volume 32, 1997, 3227-3235

18. Metal Hand Book vol. 9 from page number 711-751.

19. Hand Book of Aluminum physical mettalurgy and processes. by George E.Totten

20. Engineering metallurgy, part 1: Applied Physical Metallurgy. By Raymond A. Higgins